

Hydrogen Fuel Cells and Storage Technology Project

Clemens Heske (lead PI-experiment)

Balakrishnan Naduvalath (lead PI-theory)

Department of Chemistry

University of Nevada, Las Vegas

Project manager: Robert F. D. Perret

UNLV Research Foundation

4/18/2008

Project ID #
STP33

Overview

Timeline

- Project start: Sept. 2005
- Project end date: Sept. 2008
- Percent complete: 86%

Budget: Five tasks at UNLV (3 on storage, 2 on fuel cells)

Total project funding: \$7,927,500

- DOE: \$6,342K
- UNLV: \$1,585,500

Funding in FY07: \$4,207,500

(\$3,366K Federal; \$841,500 UNLV)

Funding in FY08: \$0

(no-cost extension)

Barriers

Primary:

M. Hydrogen Capacity and Reversibility

N. Lack of Understanding of Hydrogen Physisorption and Chemisorption

Secondary:

B. Weight and Volume

Partners

Collaborations with UTC, Shanghai Jiaotong U, Penn State, Air Products, Rice U, Berkeley Lab, Hahn-Meitner-Institute

Project management: Bob Perret, UNLV Research Foundation

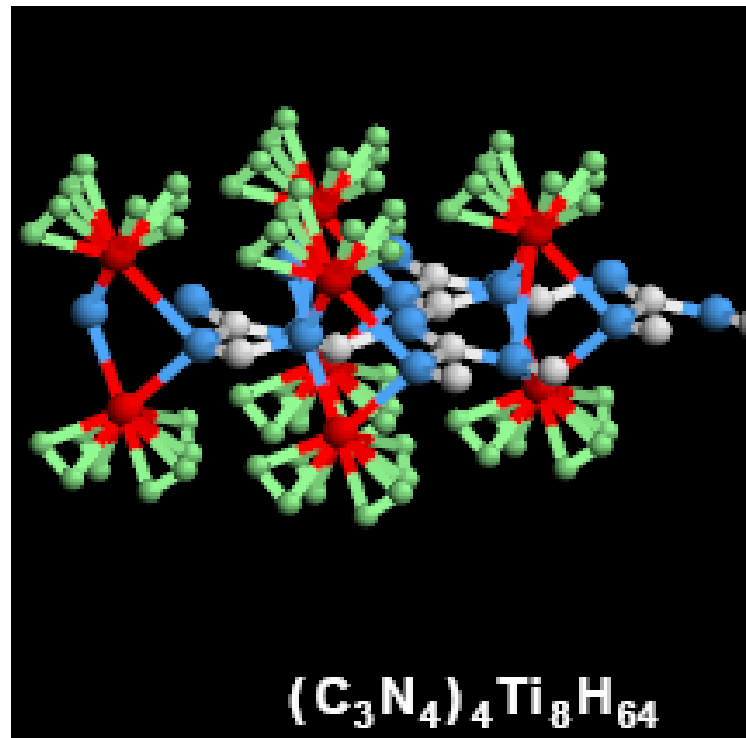
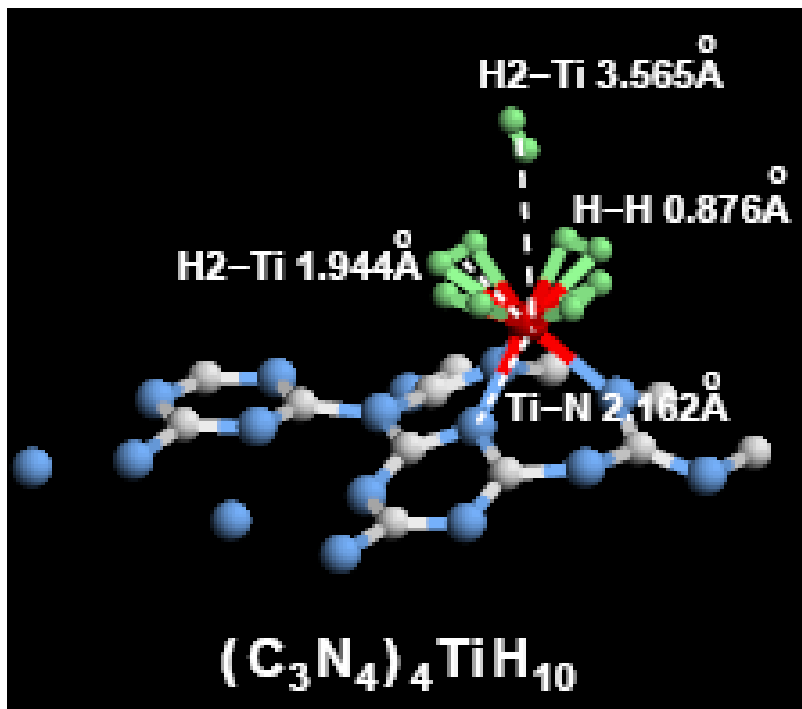
Objectives

- Perform closely-coupled theoretical and experimental investigations of
 - hydrogen adsorption/desorption in various matrices to establish a solid understanding of optimal storage concepts
 - the electronic and geometric structure of metal hydrides, nanomaterials (C, B, N, transition metals, alloys), metal adatoms, and adsorbed hydrogen molecules/atoms
 - Fuel cell membranes and catalytic materialsto predict optimized materials and structures for hydrogen storage and fuel cells in the DOE Hydrogen program
- Collaborate closely with external partners

Approach

- Task 1: Theory and Experiment of Nanomaterials for Storage Applications (New Materials, Hydrogen Uptake, Local Electronic Structure, Adsorption Energies and Geometries, ...)**
- Task 2: Metal Hydrides (Structure, Reversibility, T- and P-Dependence, ...)**
- Task 3: Mesoporous Polymer Nanostructures (Synthesis, Hydrogen Uptake, ...)**
- Task 4: Improved Fuel Cell Membrane**
- Task 5: Design and Characterization of Improved Fuel Cell Catalytic Materials**

Transition-metal decoration and hydrogen storage (Task 1)

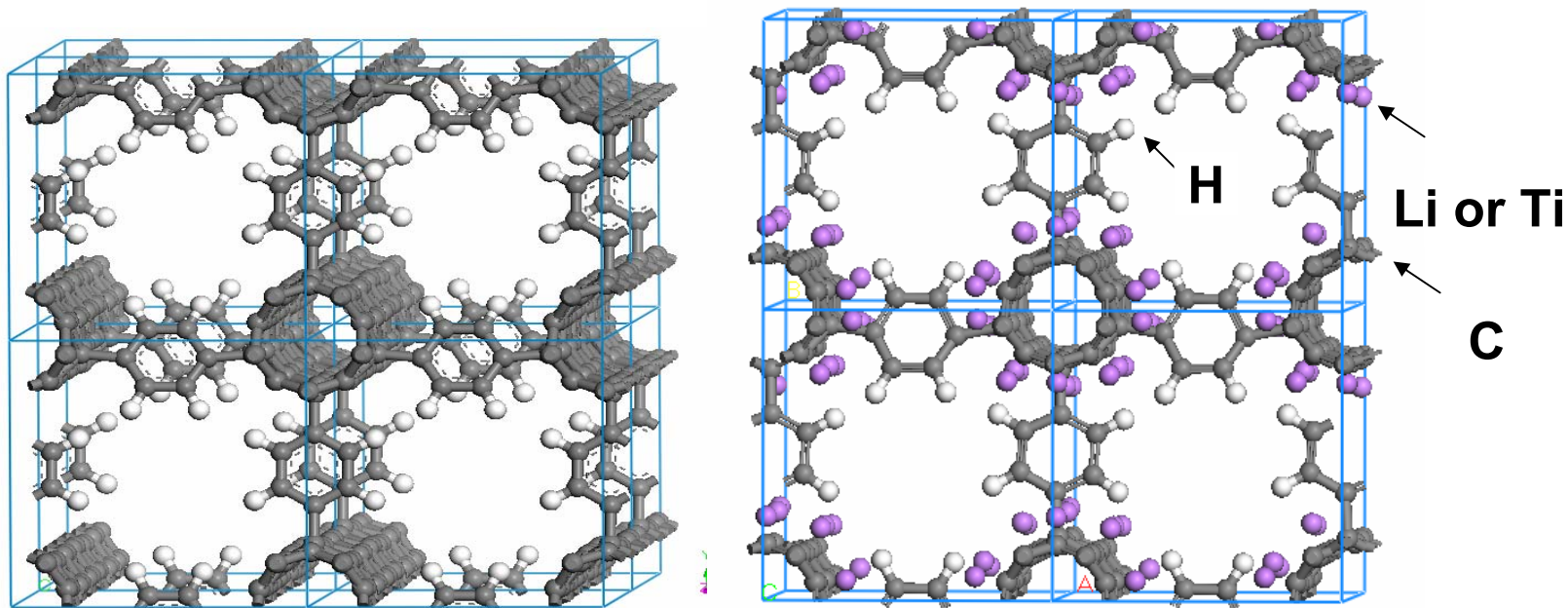


Ti	1H ₂	2H ₂	3H ₂	4H ₂	5H ₂
E (eV/H ₂)	0.60	0.36	0.39	0.09	0.02

The binding energy of H₂ on Sc is slightly lower than that on Ti.

- Up to 4 H₂ are adsorbed on each Ti atom with the binding energy ranging from 0.1 eV to 0.4 eV per H₂. (7.8wt% for double side coverage)

A novel class of 3D nanoframeworks based on CNTs (Task 1)

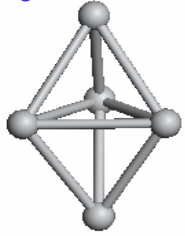


- Car-Parrinello molecular dynamics simulations indicate that the proposed frameworks are thermodynamically stable up to 20 ps at 300 K and 2 ps at 600K
- The Li-decorated 3D nanoframework is stable up to 20 ps at 300 K
- Preliminary results indicate that the Li-decorated 3D nanoframeworks are promising for hydrogen storage

Electronic structure of Titanium clusters (Task 1)

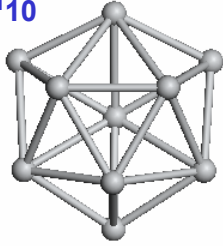
- Ti_n clusters evolve on **Pentagonal** growth pattern
- Second energy difference indicates Ti_7 and Ti_{13} clusters are highly stable, which agrees well with the experimental results

Ti_5



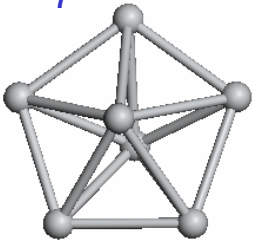
1.8694 eV

Ti_{10}



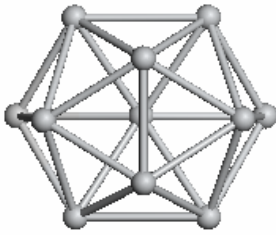
2.5187 eV

Ti_7



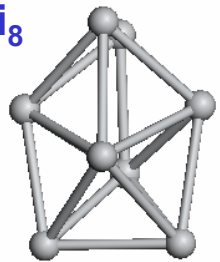
2.3128 eV

Ti_{11}



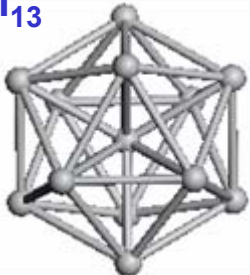
2.5700 eV

Ti_8



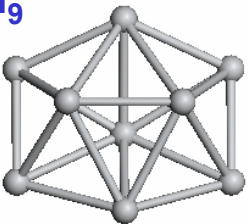
2.3562 eV

Ti_{13}



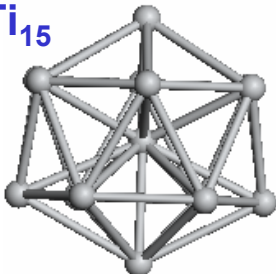
2.8063 eV

Ti_9



2.4472 eV

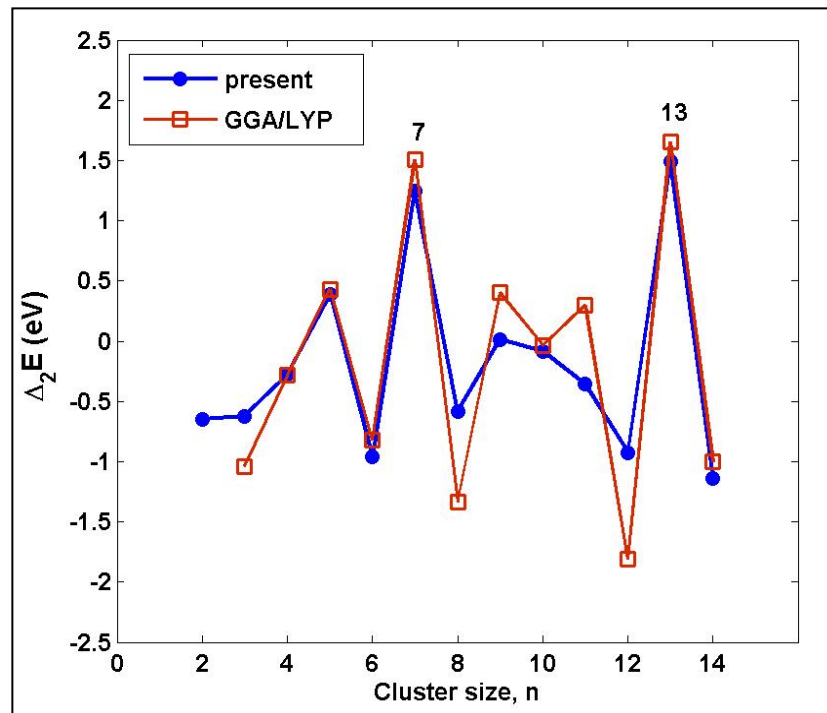
Ti_{15}



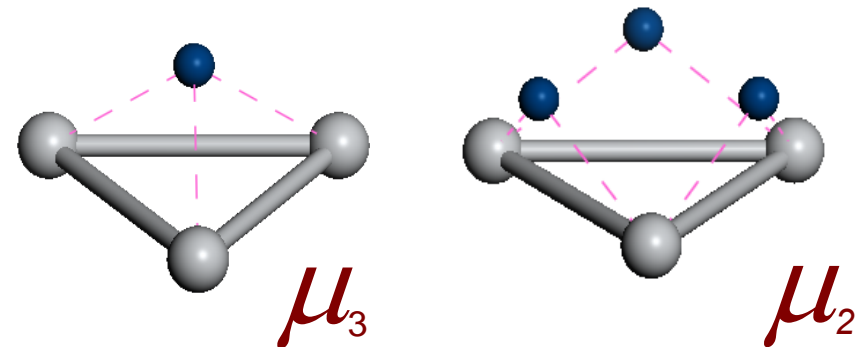
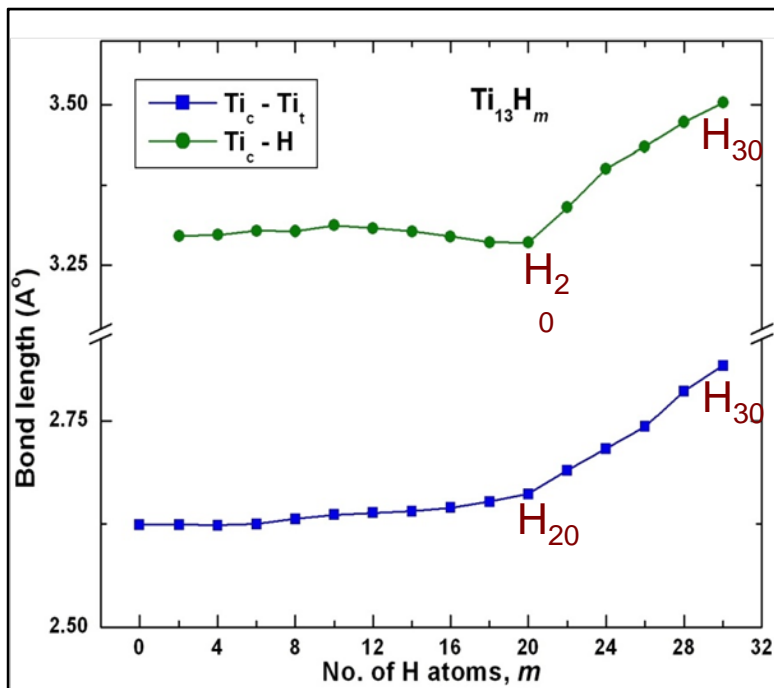
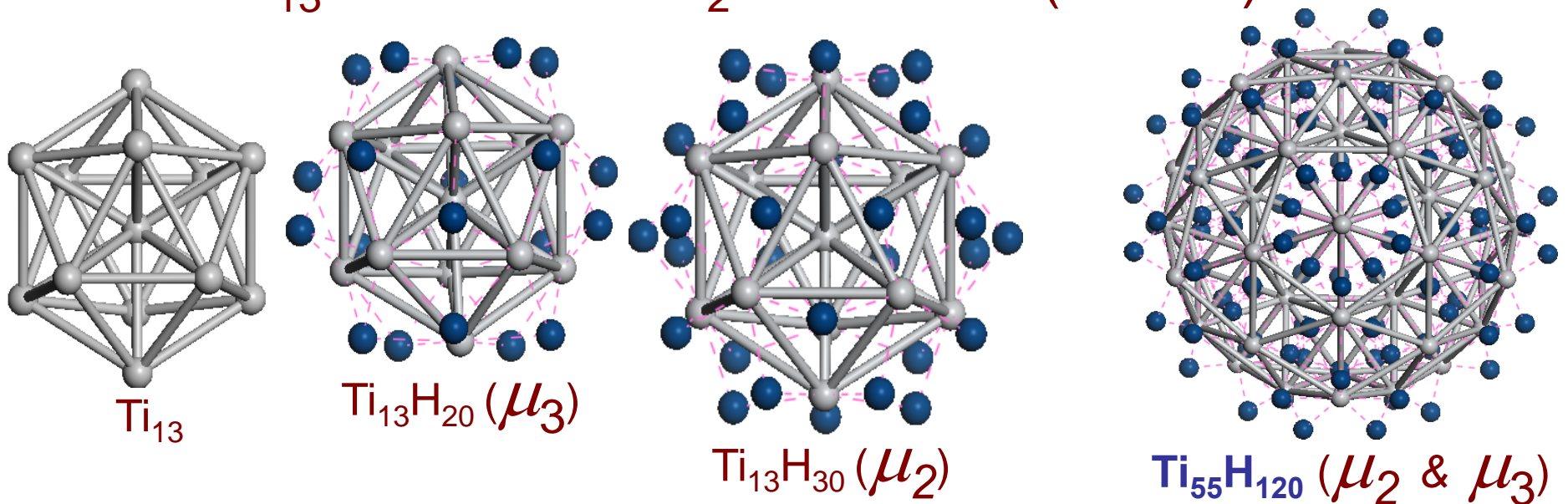
2.9270 eV

Second Energy Difference

$$\Delta_2 E = E(n+1) + E(n-1) - 2E(n)$$

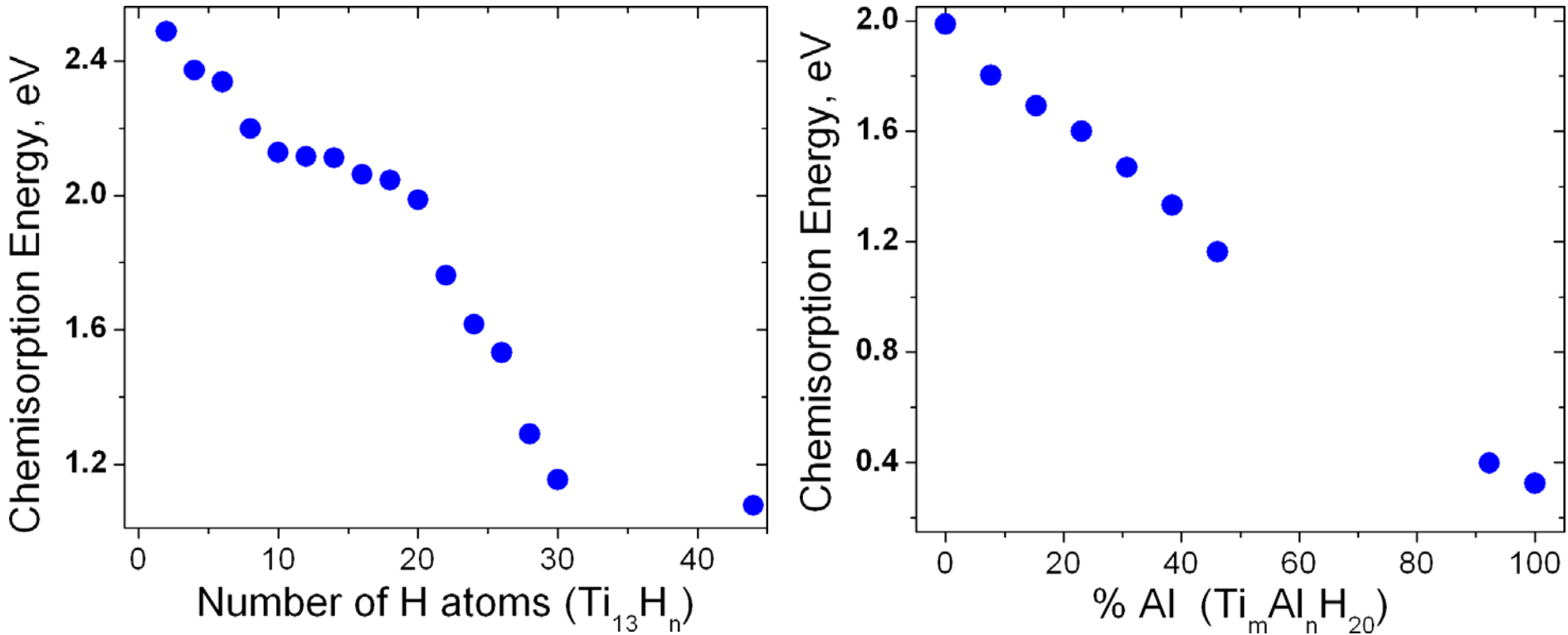


Ti₁₃ cluster and H₂ saturation (Task 1)



- Hydrogen multi-center bonds in Ti_{13}H_m
- μ_3 for $m \leq 20$ and μ_2 in $\text{Ti}_{13}\text{H}_{30}$
- Cage expansion due to saturation from $m = 20 - 30$ by 6%

The effect of alloying (Task 1)



Hydrogen Saturation or Metal Doping (Aluminum) modulates the magnitude of the chemisorption energy¹.

$${}^1E(\text{eV}) = [2/k \times [E(\text{Ti}_m\text{Al}_n) + k/2(E(\text{H}_2)) - (E(\text{Ti}_m\text{Al}_n\text{H}_k))]]$$

Surface and interface spectroscopy/microscopy of nanomaterials for hydrogen storage (Task 1)

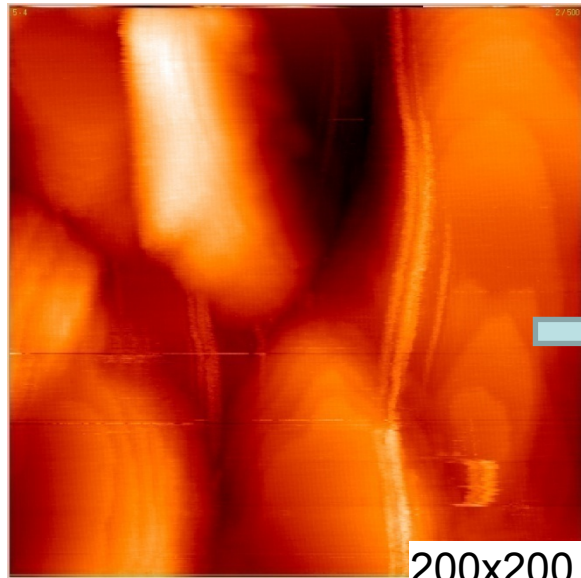
Experiment matrix for Hydrogen storage on (metal-decorated) carbon nanomaterials:

- Carbon (nano)materials: C60, SWNT, HOPG
- Metal (co-)adsorbates: Ti, Li
- Hydrogenation: molecular, atomic

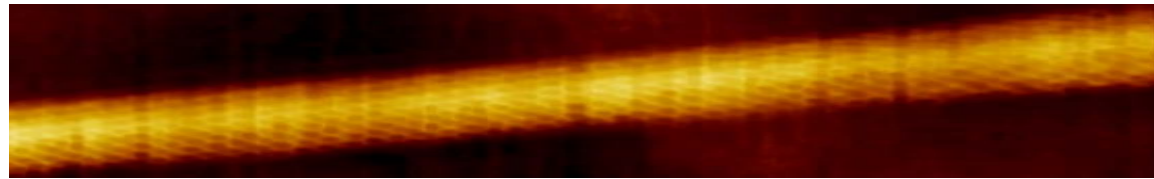
Findings:

1. Molecular hydrogen does not adsorb on SWNT at room temperature, but atomic hydrogen does
2. Molecular hydrogen adsorbs on Ti/SWNT at room temperature (!), and so does atomic hydrogen (as expected)
3. Atomic resolution STM images have been observed for SWNT, and first metal deposition studies have been performed
4. Atomic/molecular hydrogen source fully operational
5. Not shown (but last time): Oxidation study of Ti (with and without Li) on carbon nanomaterials

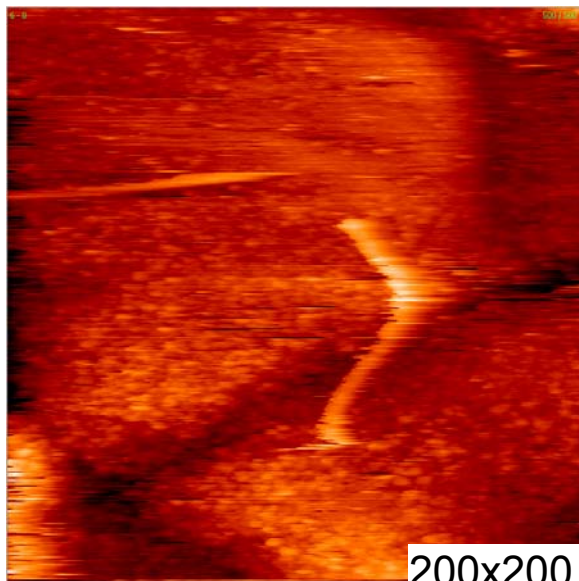
Scanning Tunneling Microscopy/Spectroscopy of SWNT with/without Ti decoration (Task 1)



200x200 nm²

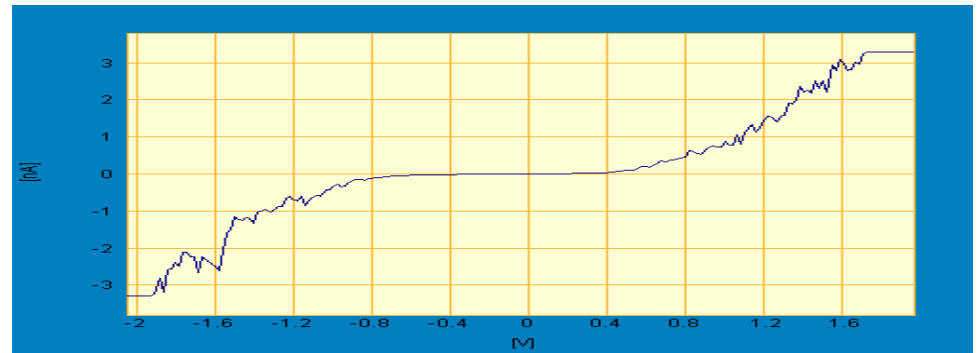


STM image of SWNT on Au with atomic resolution



200x200 nm²

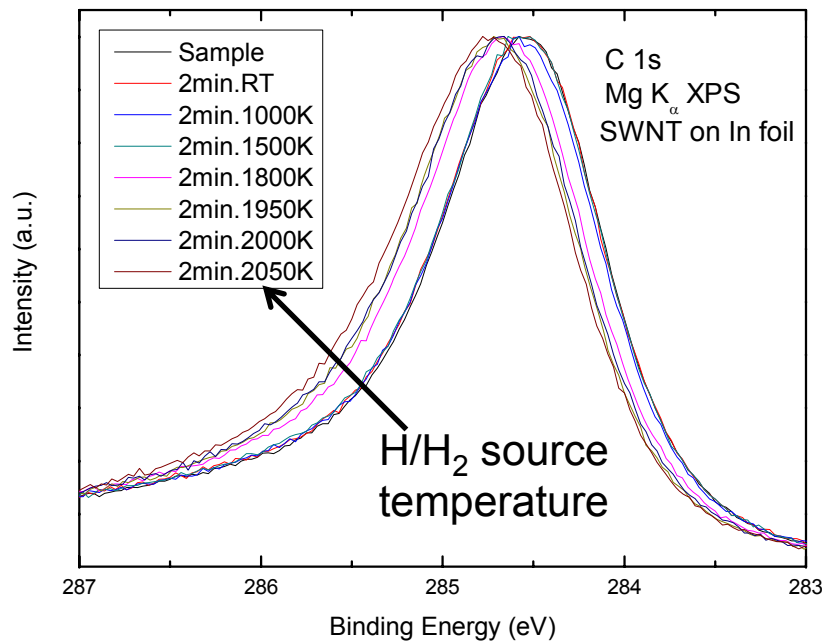
Ti deposited on top of SWNT/Au



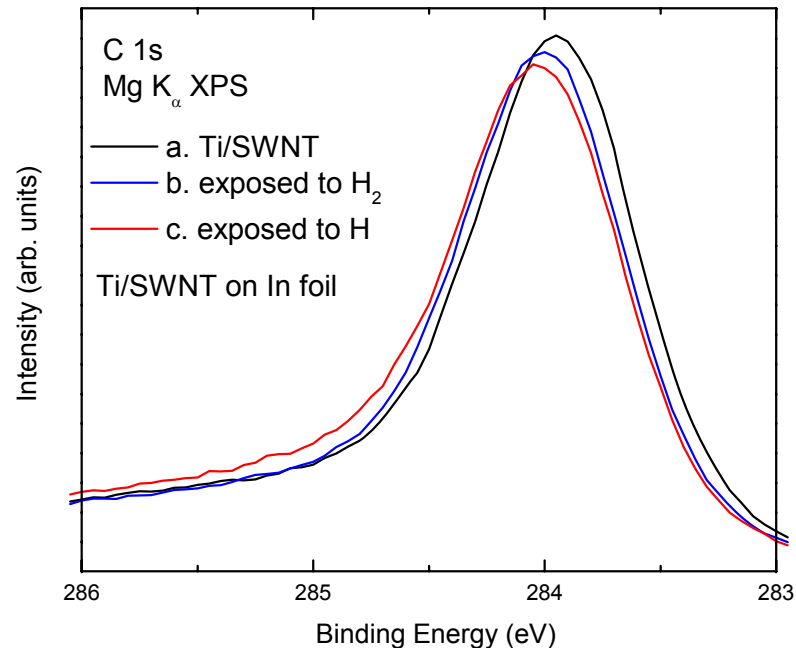
I-V curve and STS of SWNT on Au

XPS: Hydrogenation of SWNT and Ti/SWNT (Task 1)

Hydrogenation of SWNT



Hydrogenation of Ti/SWNT



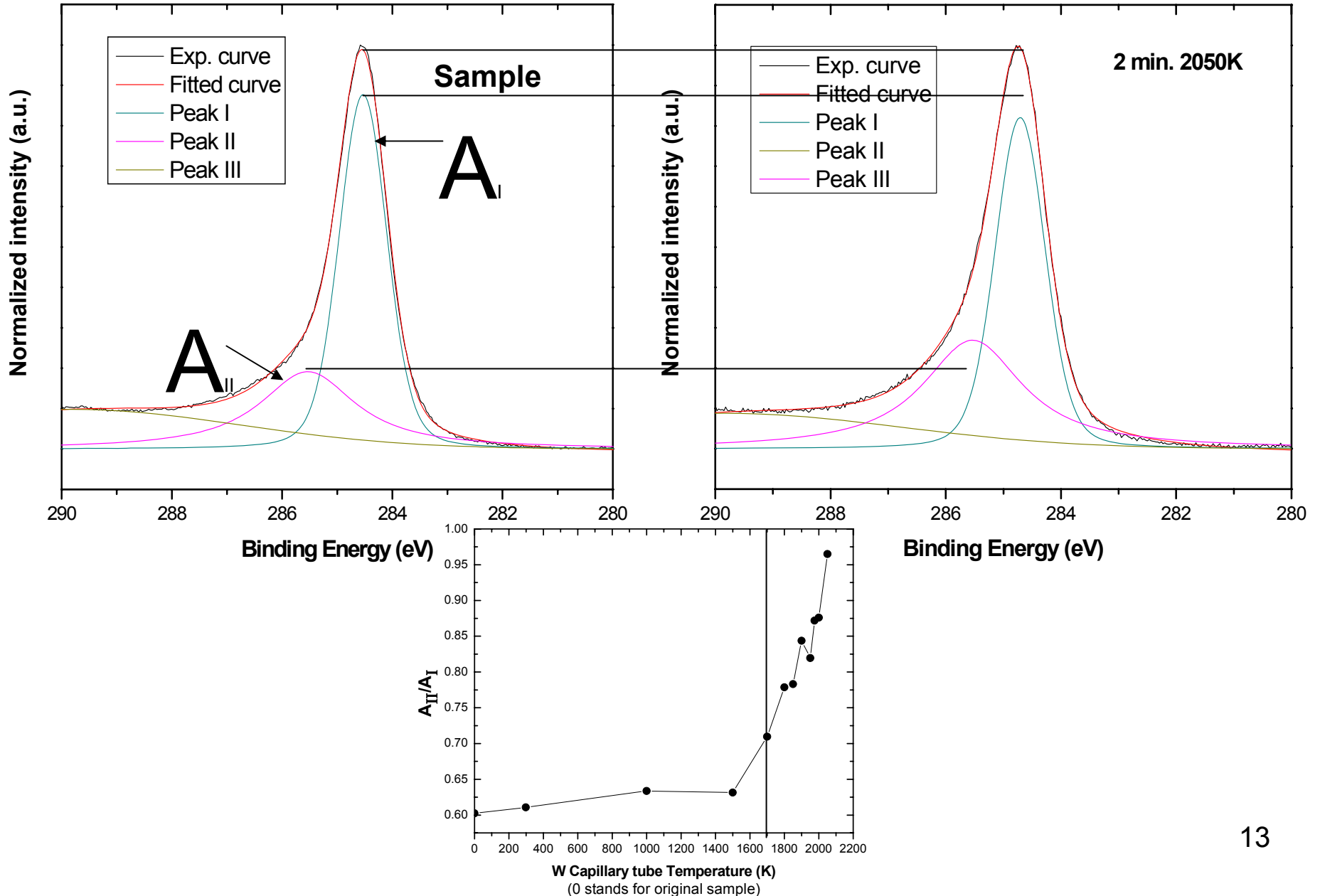
Hydrogenation of SWNT:

1. No shift in C 1s for molecular hydrogen adsorption (at RT)
2. C 1s shifts to higher binding energy for atomic hydrogen (along with capillary temperature), indicating H adsorption

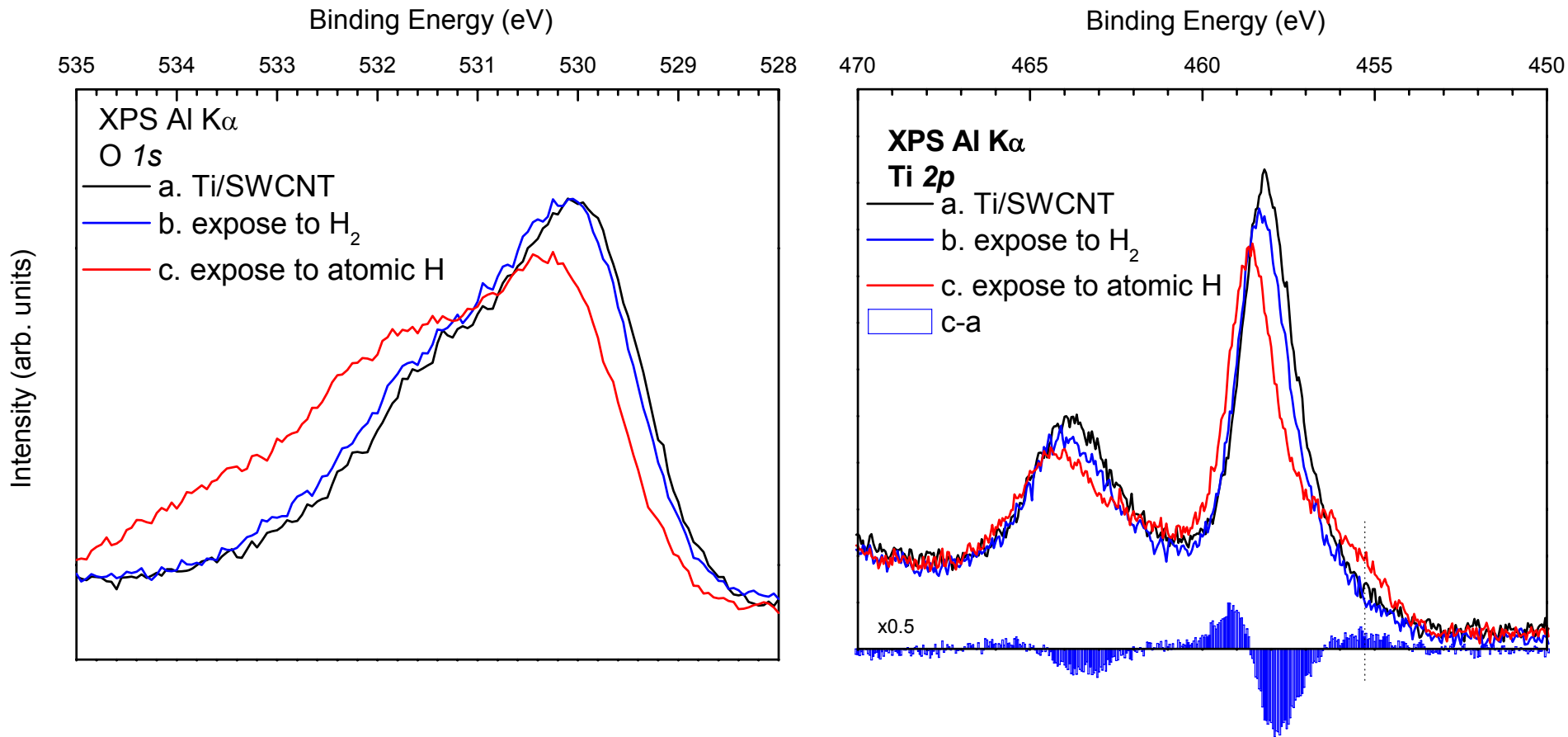
Hydrogenation of Ti/SWNT:

1. Molecular hydrogen adsorbs at RT and modifies the chemical/electronic environment of carbon!
2. Only small further enhancement for atomic hydrogen

XPS: Hydrogenation of SWNT (Task 1)



XPS: Hydrogenation of Ti/SWCNT (Task 1)



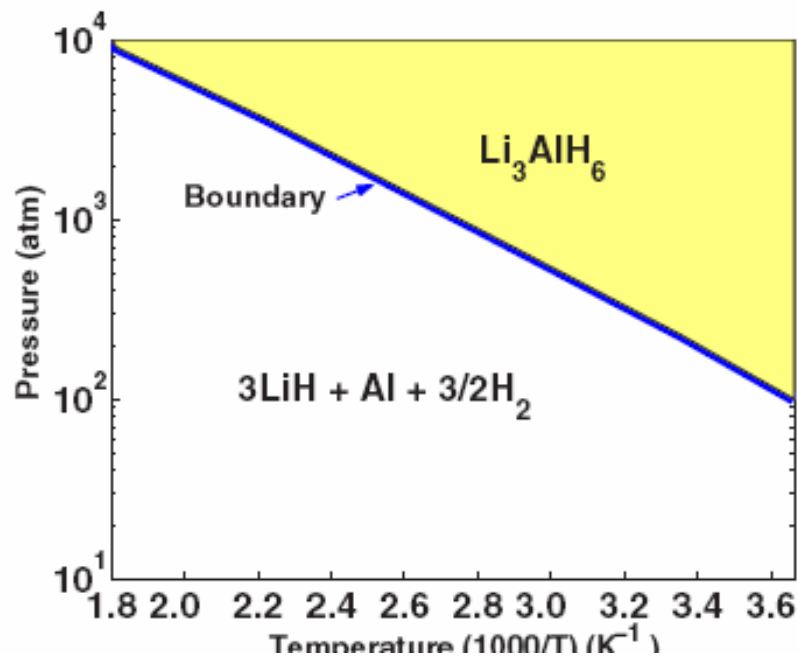
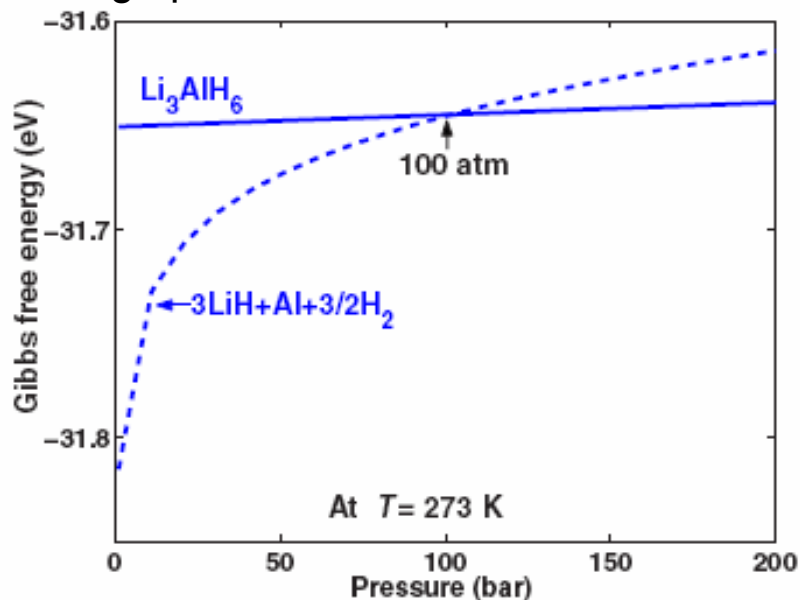
1. The O 1s core level shows a small change upon H $_2$ exposure and a more pronounced change for H exposure
2. Ti 2p changes agree with the finding of molecular hydrogen adsorption
Atomic hydrogen induces a new chemical Ti species

Gibbs free energy and temperature-pressure phase diagram of lithium alanates (Task 2)

Apply first-principles electronic structure and lattice dynamics calculations within and beyond the harmonic phonon approximation to examine the thermodynamic phase stability of lithium alanates and predict their reaction pathways and reversibility

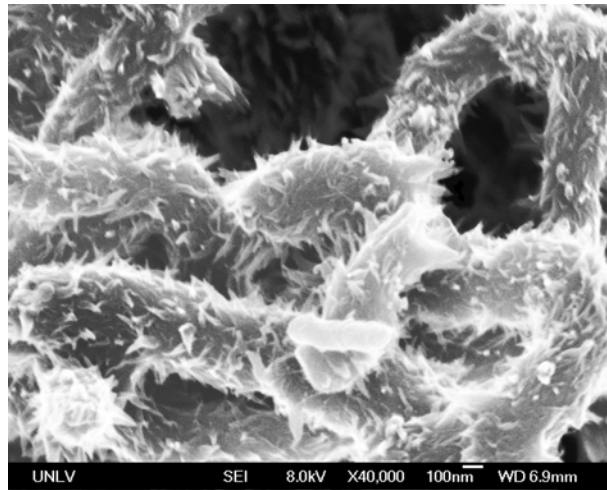
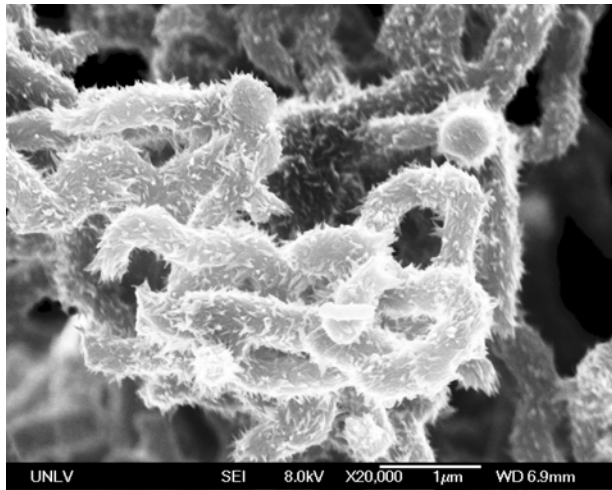
Results:

- Obtained a comprehensive set of thermodynamic functions over a wide temperature range for LiAlH_4 , Li_3AlH_6 and LiH .
- Evaluated decomposition reactions to determine reversibility and suitability for practical use in mobile applications.
- Established the thermodynamic (temperature-pressure) phase diagram for lithium alanates and identified key operating physical parameters for hydrogen storage and reversible release-recharge process.

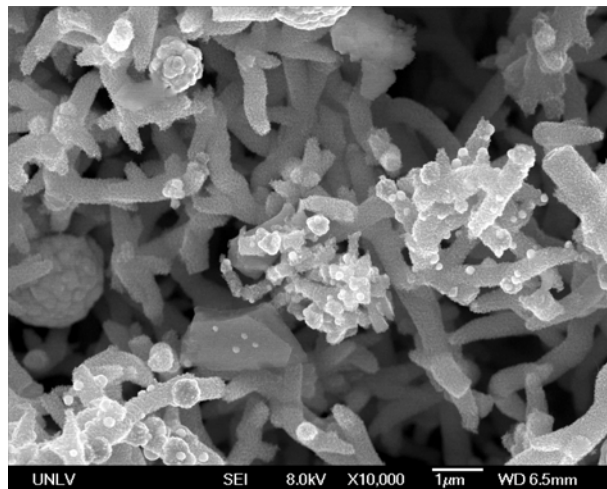
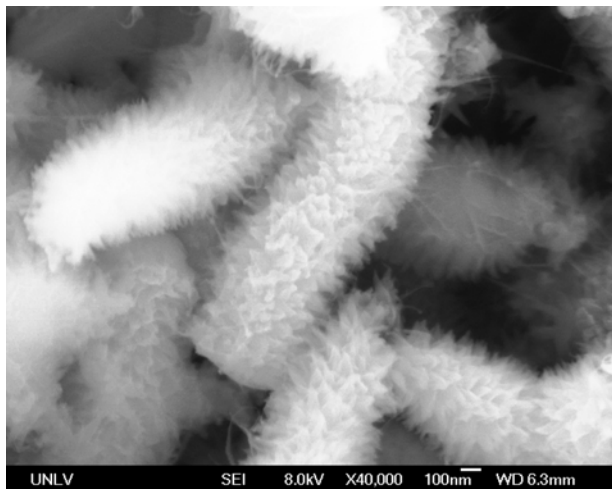


PANI/Pd Composites (Task 3)

Pd(ii) reduction in PANI



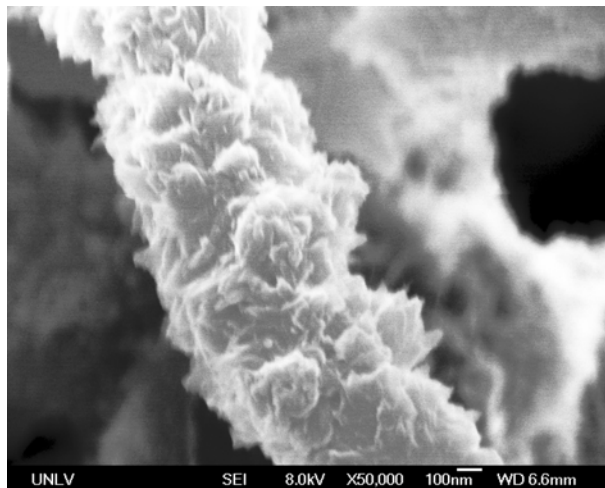
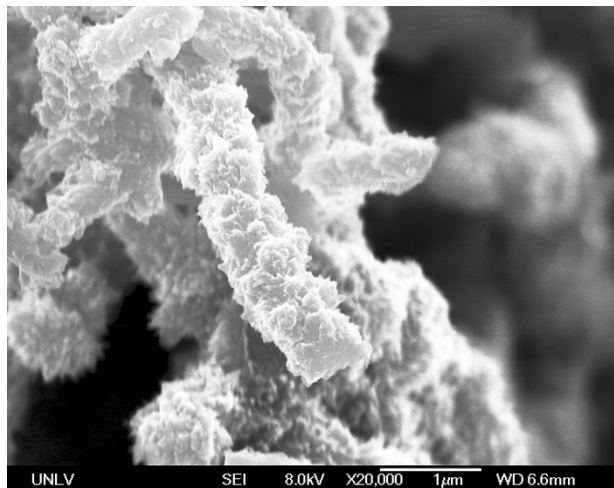
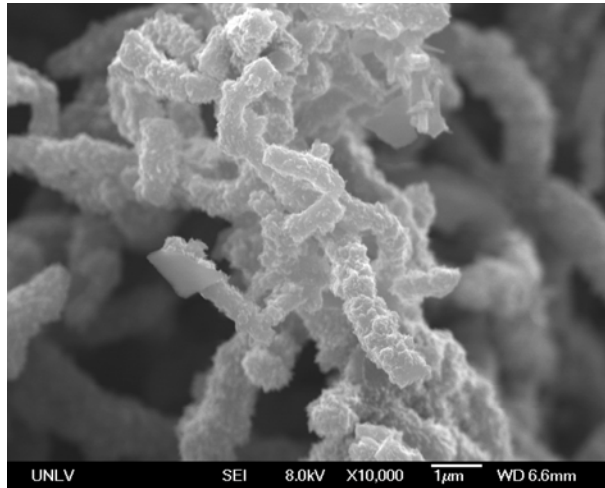
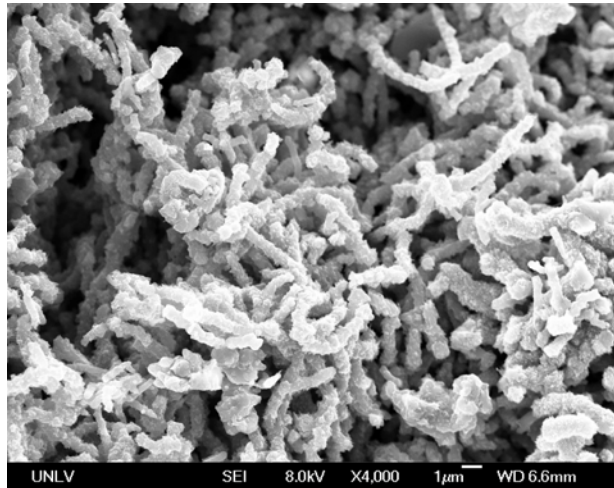
Pd morphology is a function of the number of voltammetric cycles



Pd aggregation also possible with potentiometric growth

PANI/Pd Composites (Task 3)

Pd(IV) Reduction in PANI



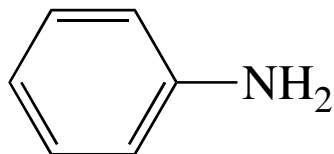
Pd thickness is a function of the number of voltammetric cycles

Pd Loading in Composite Materials (Task 3)

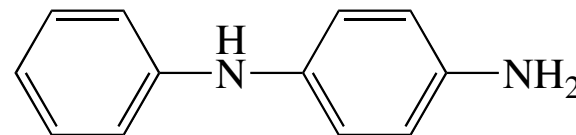
Chemical Synthesis

% Mass Loss (TG)	A	B	C	D	E	F	G	H
	71.75	72.88	73.59	70.99	88.81	79.21	91.02	84.54
	75.60	75.26	72.68	71.09	86.18	77.61	91.06	87.47
4th trial	71.12	70.94	72.66	71.03	92.27	78.91	92.08	88.46
	78.15	73.70	75.79		89.92	80.21	95.50	89.12
Average	74.16	73.20	73.68	71.04	89.30	78.99	92.42	87.40
Standard Deviation	3.32	1.80	1.47	0.05	2.53	1.07	2.11	2.02
RSD	4.48	2.46	2.00	0.07	2.83	1.36	2.29	2.31
Pd content in %	25.85	26.81	26.32	28.96	10.71	21.02	7.59	12.60

Monomer (Anilin)

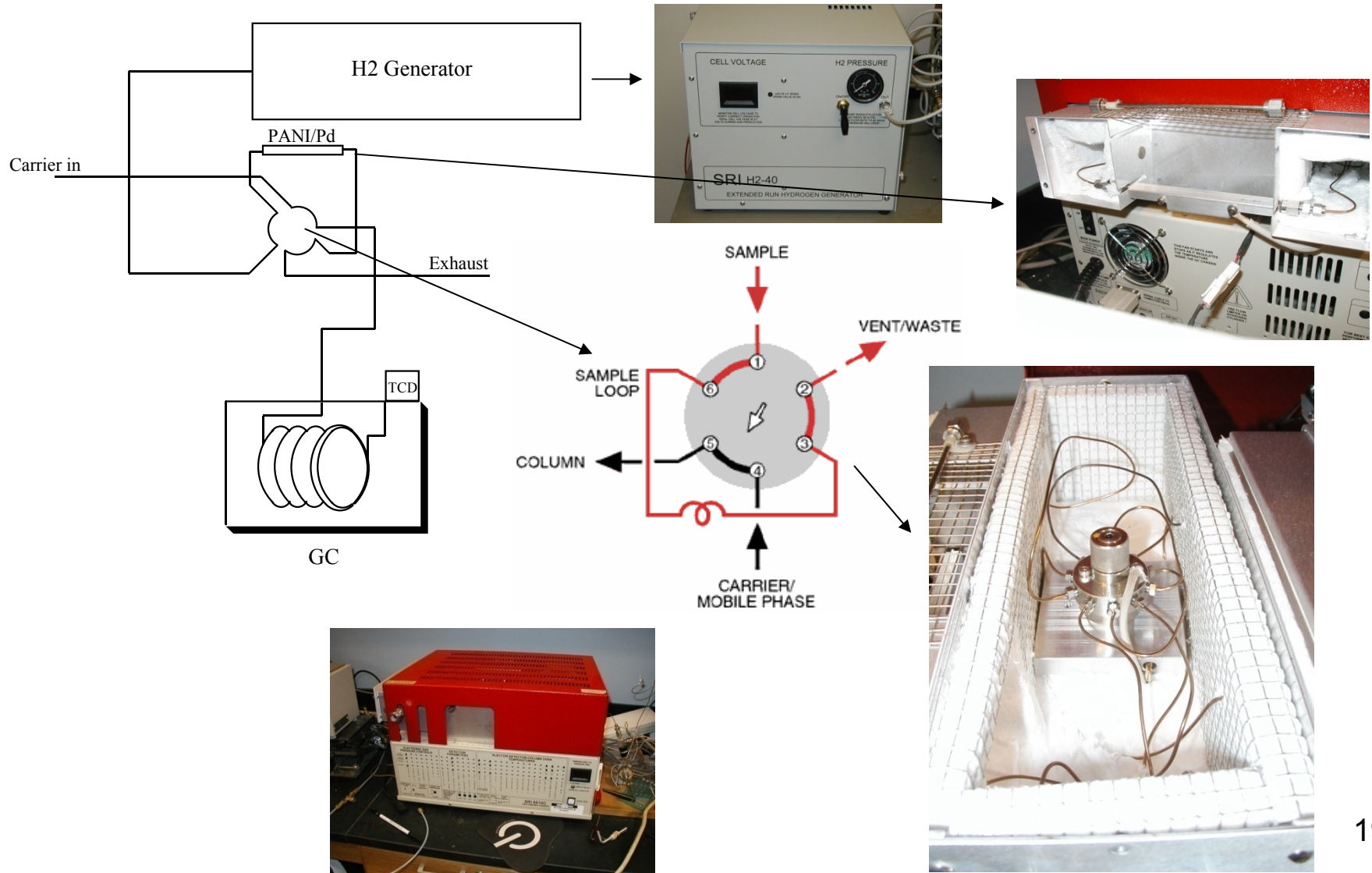


Dimer (NPPD)



The materials produced using monomer had more Pd regardless of anion oxidation state
Pd loading is between ~10 – 30%.

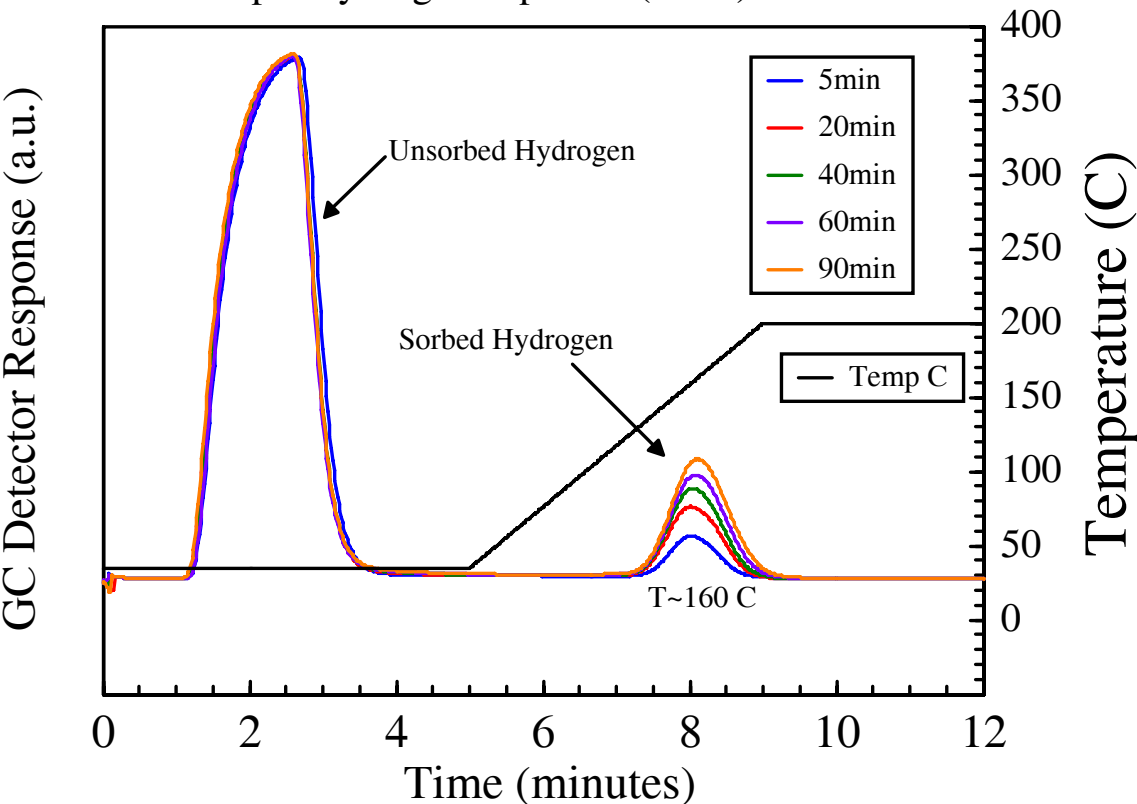
H Sorption Apparatus (Task 3)



Hydrogen Sorption in Chemical Composites (Task 3)

Material A

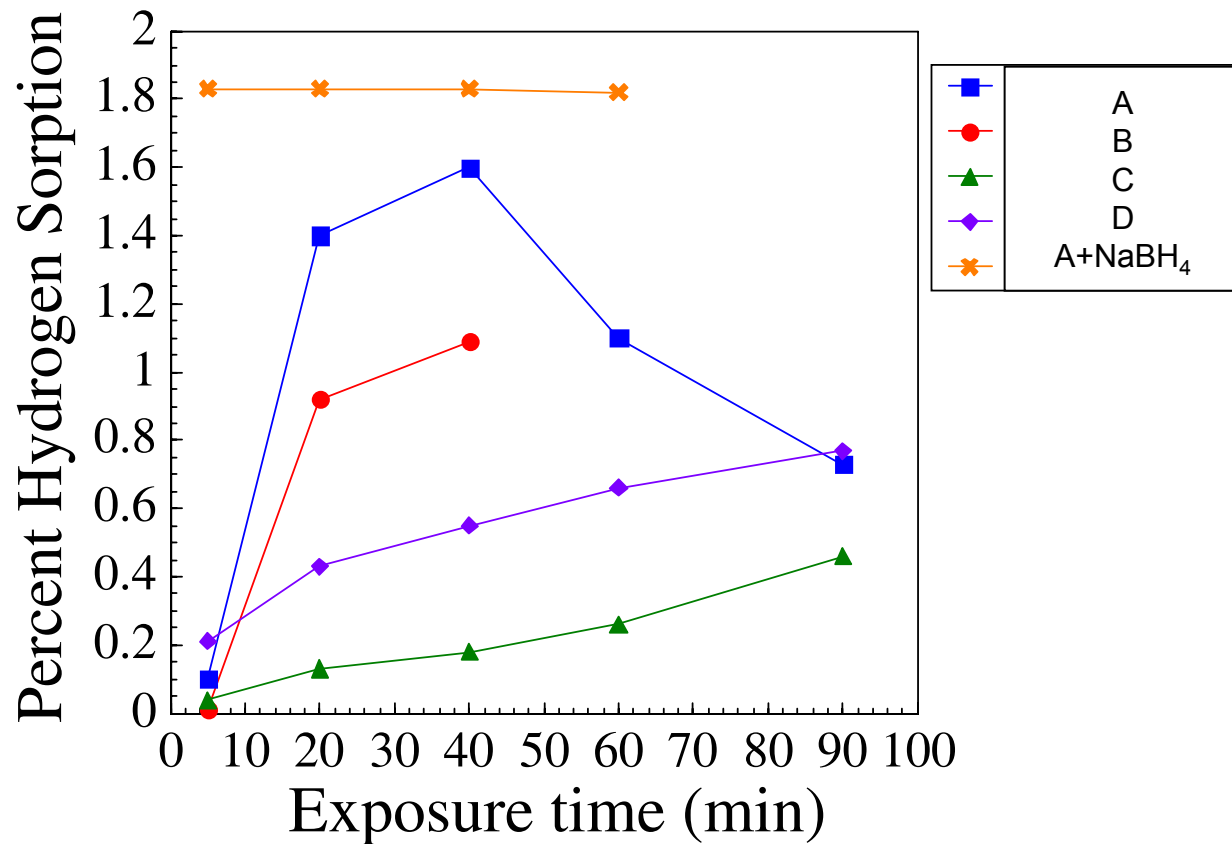
30 psi Hydrogen exposure (static)



Sorption is obtained using a normal GC with a hydrogen generator

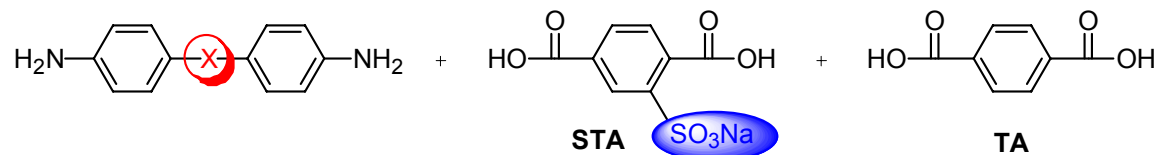
- **The first peak remains unchanged relative to the second because it represents the void volume of hydrogen in the tube rather than sorbed hydrogen**
- **The second peak represent sorbed hydrogen**
- **A temperature ramp is used to observed desorption**

Hydrogen Sorption Results and Conclusions (Task 3)

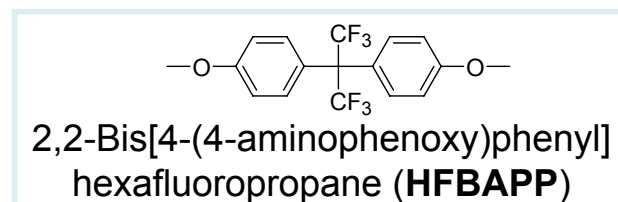
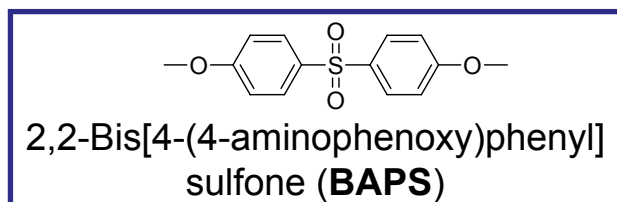
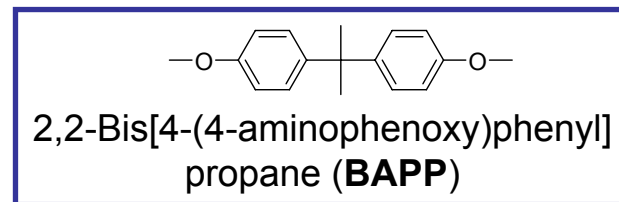
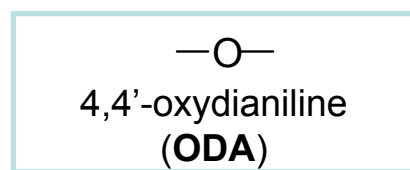
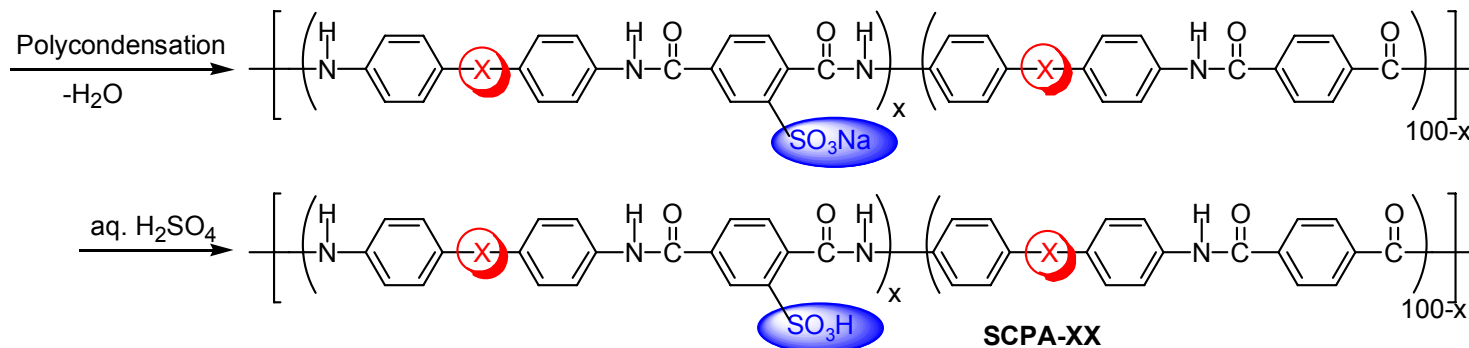


- Five composite materials have been produced that show promise for Hydrogen sorption
- Preliminary measurements have been made to verify the sorption properties
- Variations in the chemical composites have been eliminated by treatment with NaBH₄ thus reducing any unreduced species
- This material shows the highest sorption suggesting that treatment of the other chemically prepared composites may increase sorption properties

Development of New Sulfonated Aromatic Polymers for Proton Exchange Membrane Fuel Cell Applications (Task 4)



Synthesis of Sulfonated Polyamides



Characterization of Sulfonated Polyamide PEMs (Task 4)

Intrinsic viscosity, IEC and EW of sulfonated polyamides

Polymer ^a	Intrinsic Viscosity (dL/g)	IEC (mequiv/g)		EW (g/mol SO ₃)
		expt	calcd	calcd
ODA-SCPA-40	2.08	1.10	1.05	950
ODA-SCPA-50	1.86	1.34	1.33	752
ODA-SCPA-60	2.17	1.58	1.56	640
ODA-SCPA-70	2.78	1.80	1.83	546
BAPP-SCPA-70	1.86	1.17	1.06	945
BAPS-SCPA-70	1.76	1.13	1.11	898
HFBAPP-SCPA-70	1.40	0.99	0.94	1066

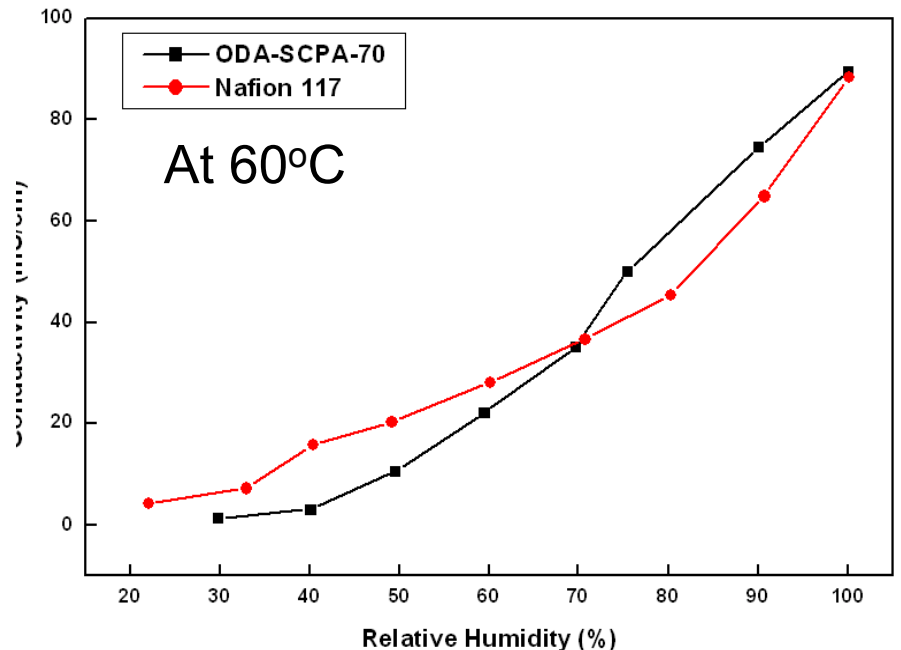
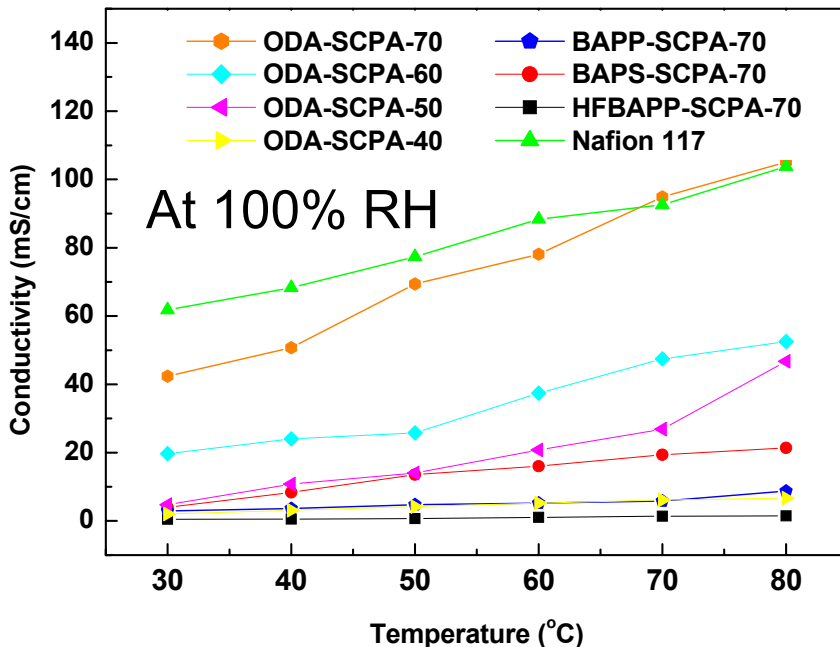
^a Number means the degree of sulfonation

Properties of Sulfonated Polyamide PEMs (Task 4)

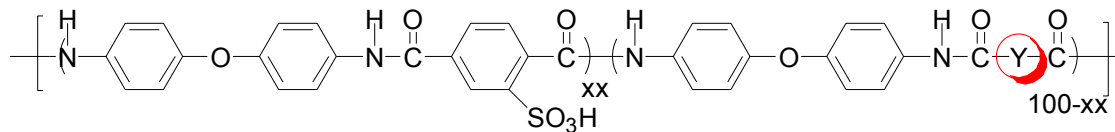
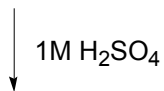
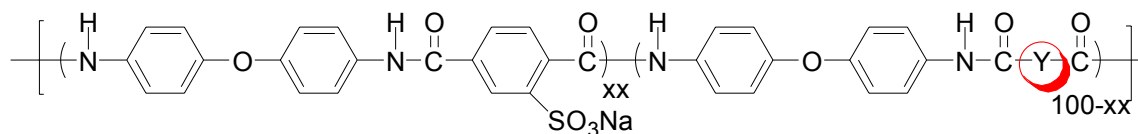
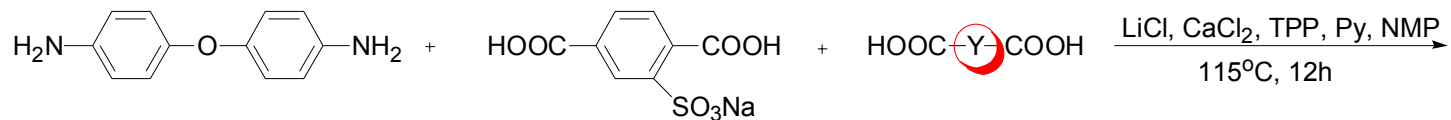
Water uptake and oxidative stability of sulfonated polyamides

Polymer	Water Uptake (%)	Oxidative stability	
		τ_1 (min)	τ_2 (min)
ODA-SCAP-40	17%	50	110
ODA-SCPA-50	23%	45	100
ODA-SCPA-60	24%	45	95
ODA-SCPA-70	33%	55	120
BAPP-SCPA-70	17%	65	150
BAPS-SCPA-70	10%	70	165
HFBAPP-SCPA-70	13%	135	260

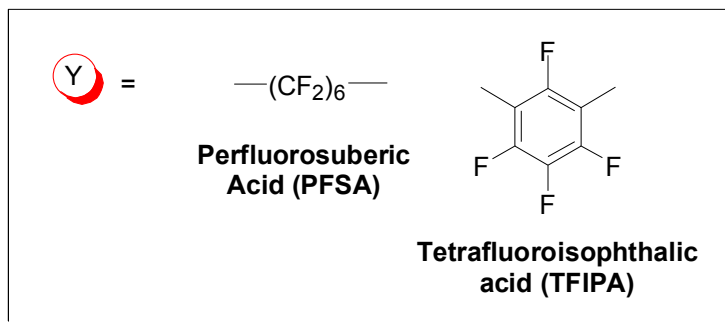
τ_1 : elapsed time when the membrane starts to become brittle in Fenton's reagent
 τ_2 : elapsed time when the membrane starts to dissolve in Fenton's reagent



Synthesis of Sulfonated Fluoropolyamides (Task 4)



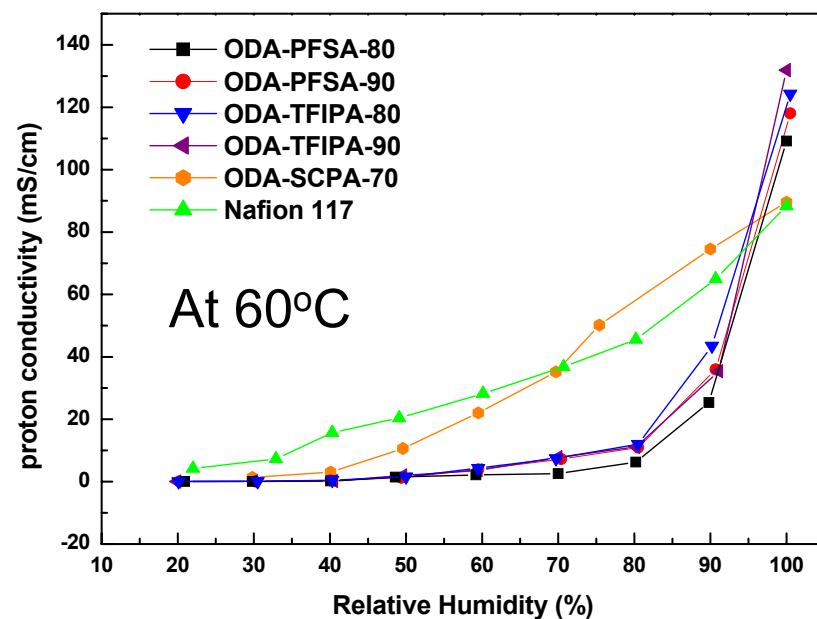
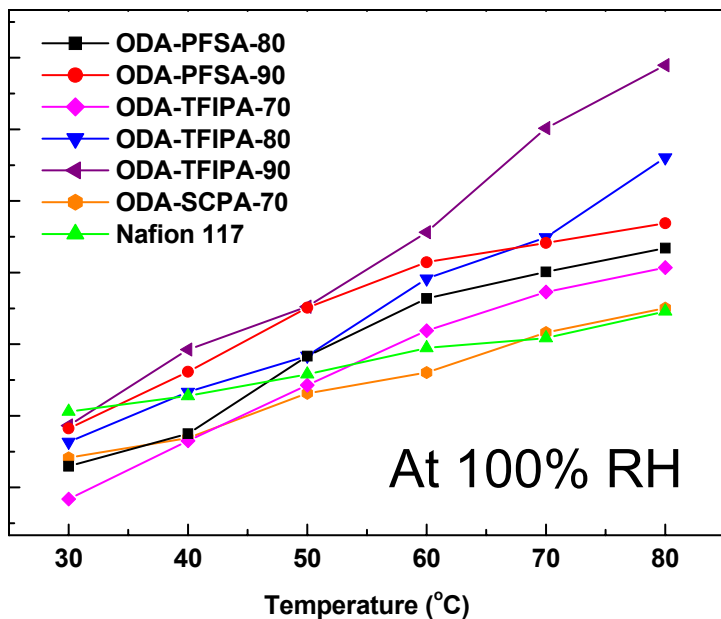
ODA-PFSA-XX or ODA-TFIPA-XX



Properties of Sulfonated Fluoropolyamide PEMs (Task 4)

Intrinsic viscosity, IEC and water uptake of sulfonated fluoropolyamides

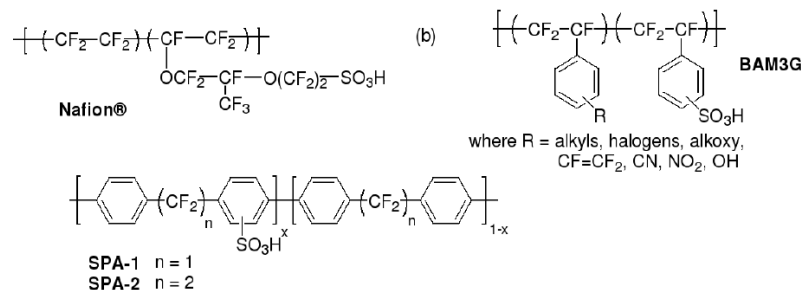
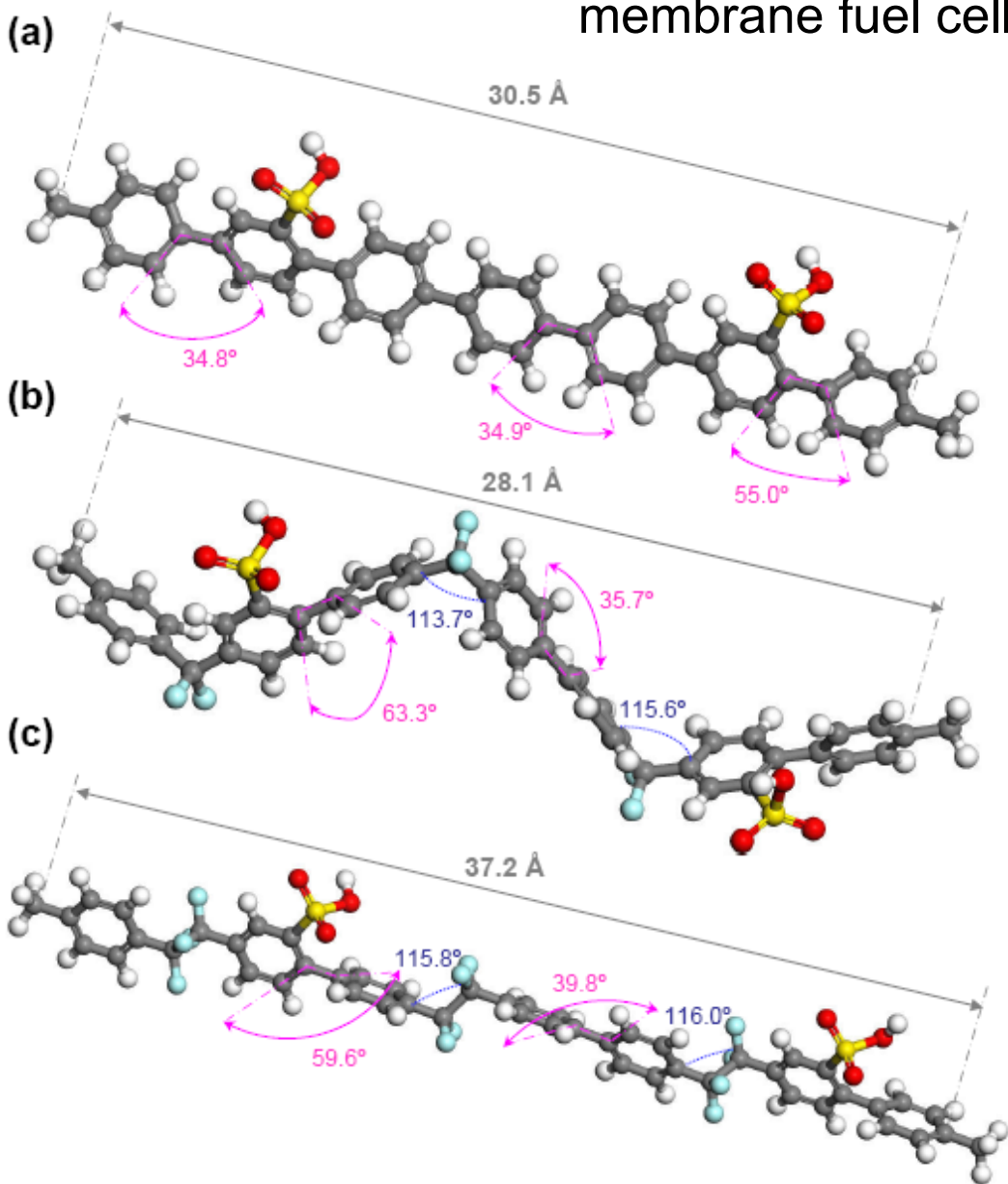
Polymer ^a	Intrinsic Viscosity (dL/g)	IEC (mequiv/g)		Water Uptake (wt %)
		exp	calc	
ODA-PFSA-80	1.24	1.74	1.72	8
ODA-PFSA-90	1.50	1.99	2.00	31
ODA-TFIPA-70	1.45	1.61	1.65	20
ODA-TFIPA-80	1.37	1.81	1.87	39
ODA-TFIPA-90	1.35	2.05	2.09	41



Summary and Current Status of Membrane Polymer Development (Task 4)

- A Novel class of high molecular weight sulfonated copolyamides were synthesized via polycondensation of sulfonated terephthalic acid and diamine monomer
- The sulfonated copolyamides had lower water uptake which could be potentially used as fuel cell membrane
- The ODA-based sulfonated polyamides (ODA-SCPA-70) displayed high proton conductivity (100 mS/cm) which is comparable to that of Nafion 117
- New partially fluorinated sulfonated copolyamides were synthesized and they showed higher proton conductivity (130-140 mS/cm) than Nafion at 80°C/100% relative humidity

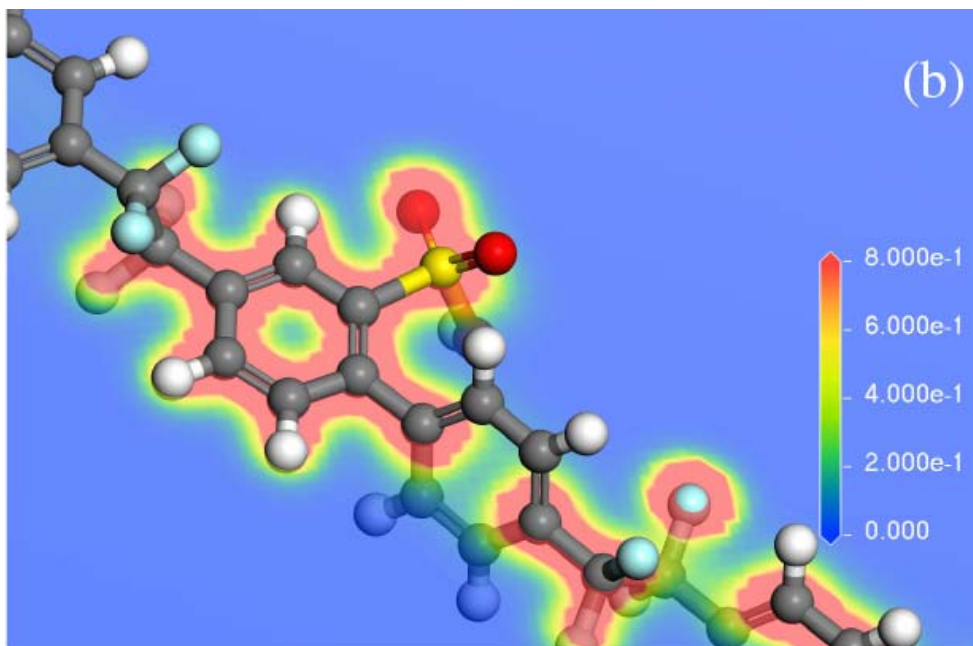
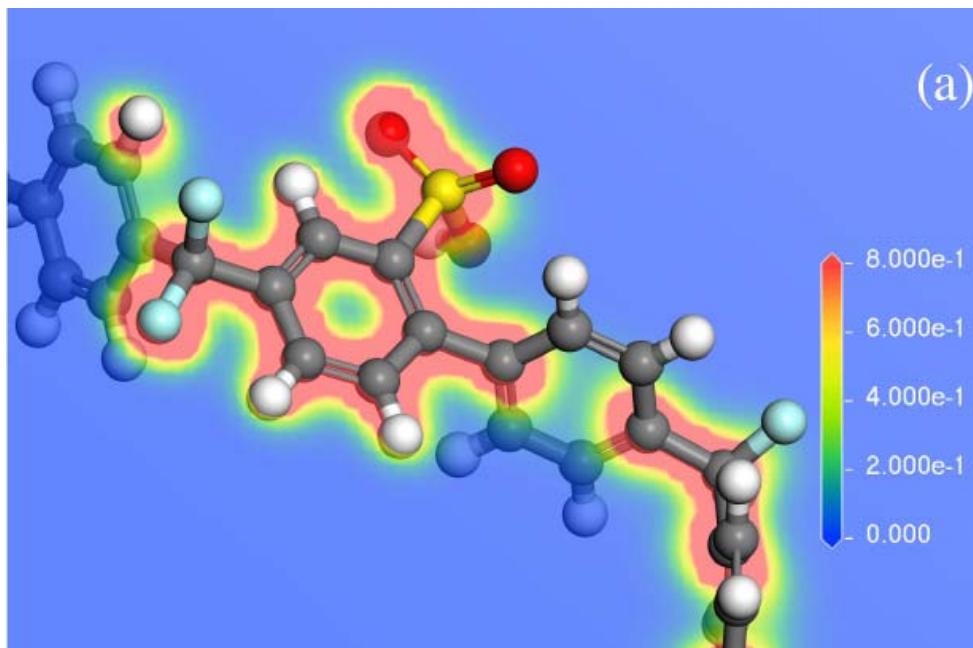
Nanoscale building blocks for the development of novel proton-exchange membrane fuel cells (Task 4)



Top: Chemical structures of proton exchange membranes: (a) Nafion (DuPont), (b) BAM3G (Ballard Advanced Materials), (c) proposed SPA-1 and SPA-2 sulfonated polyarylenes

Left: Fully optimized geometries of dry fragments of: (a) a reference SPA-1/SPA-2-analog polymer without difluoromethylene units along the backbone, (b) SPA-1 polymer, (c) SPA-2 polymer. Carbon (grey); oxygen (red); hydrogen (white); fluorine (light blue).

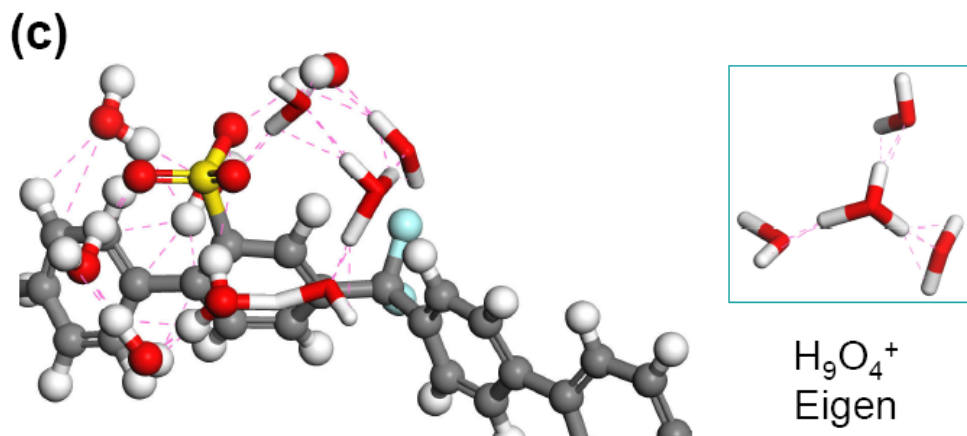
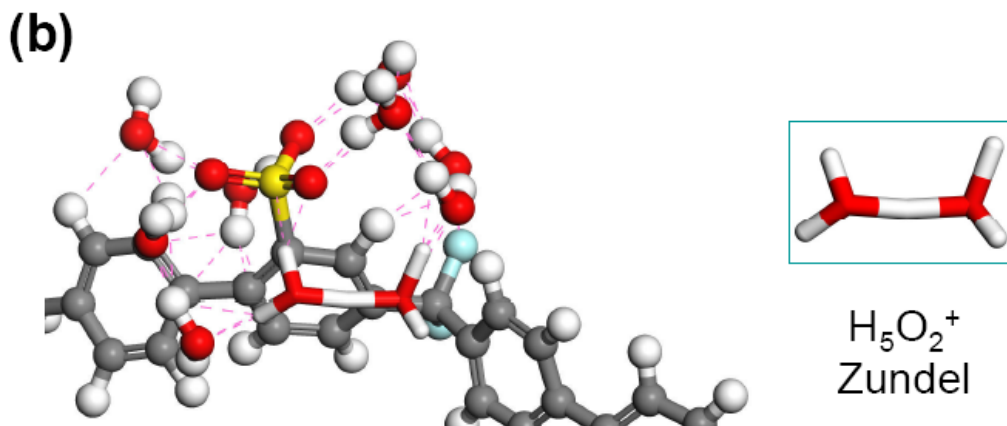
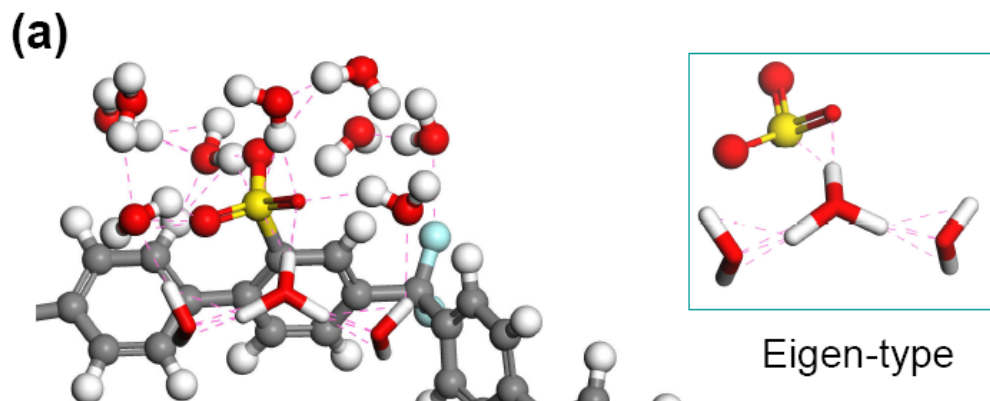
Nanoscale building blocks for the development of novel proton-exchange membrane fuel cells (Task 4)



Calculations were performed using density functional theory. Exchange correlation energy calculated using the generalized gradient approximation (GGA) with the parametrization of Becke-Lee-Yang-Parr (BLYP). The Γ point was used to represent the Brillouin zone. Double numerical basis sets including polarization functions on all atoms (DNP) in the calculations.

Left: Projected electronic charge densities of (a) SPA-1 and (b) SPA-2 polymeric fragments. Charge densities are plotted in $e/\text{\AA}^3$ units. The calculated charge density is continuous and uniformly distributed along the aryl-SO₃H bond and the backbone.

Nanoscale building blocks for the development of novel proton-exchange membrane fuel cells (Task 4)



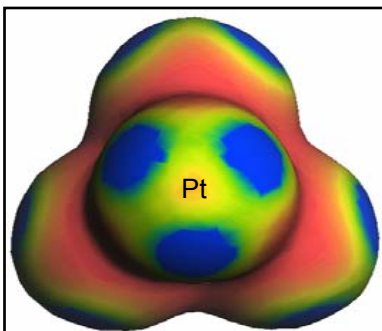
Snapshots of molecular dynamics simulations showing the proton transport mechanisms in the vicinity of hydrated sulfonic acid protogenic groups of the SPA-1 fragment at 300 K. The snapshots correspond to: (a) 0.1 ps, (b) 0.7 ps, and (c) 1.1 ps. Dashed lines depict the hydrogen-bonded network of water molecules.

Effect of Co doping on the catalytic activity of Pt clusters (Task 5)

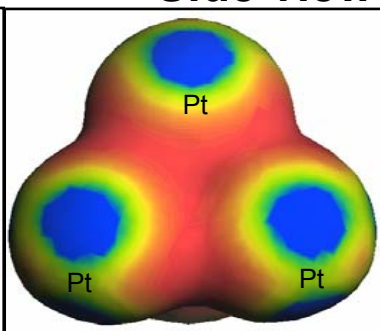
Electrostatic Potential Map

(a) Pt₄

Top view

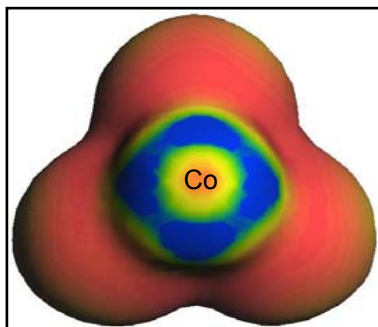


Side view

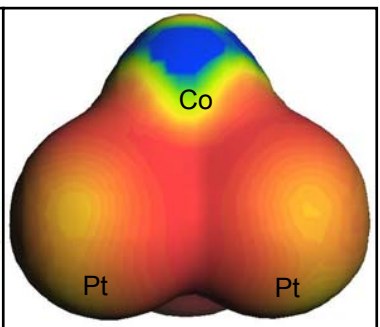


(b) Pt₃Co

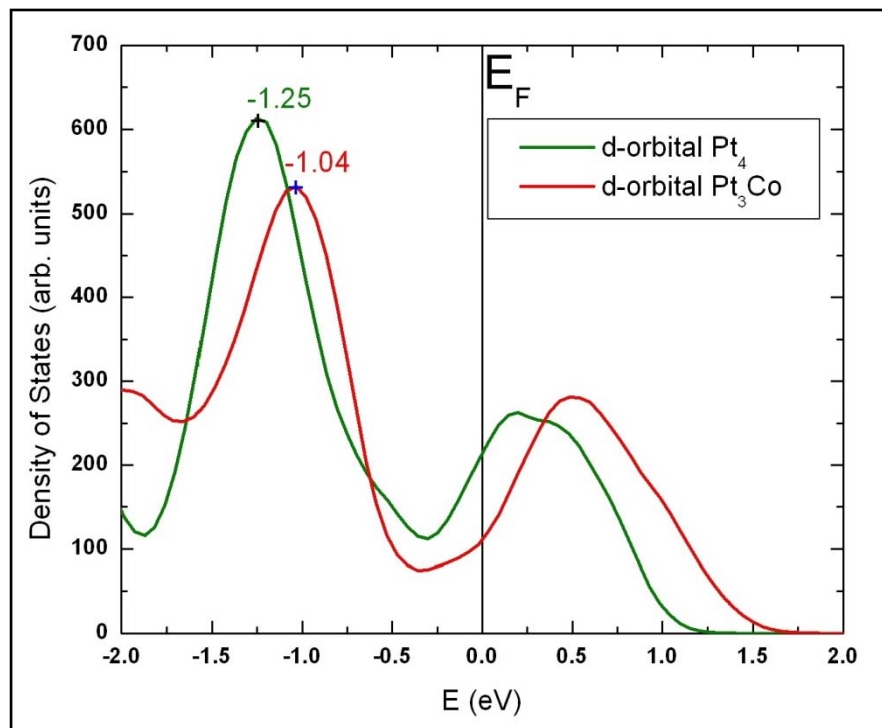
Top view



Side view

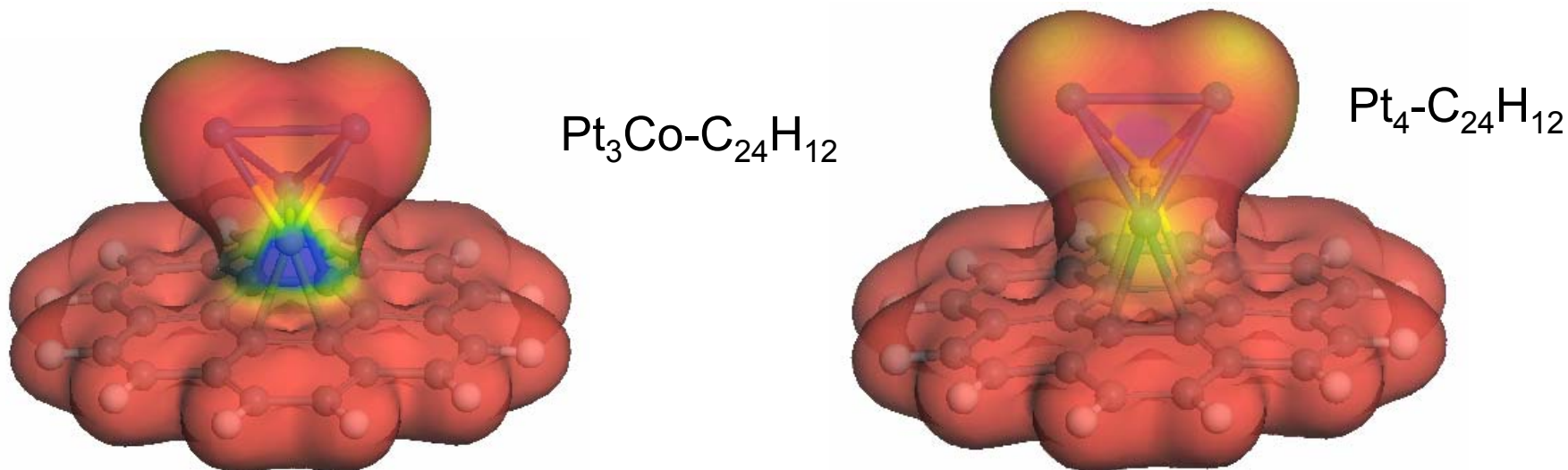


Total Density of States of Pt₄ and Pt₃Co



Position of the d-band relative to the Fermi-level has important consequences for the catalytic activity

Catalyst support interaction: O₂ and CO adsorption on Coronene supported Pt₄/Pt₃Co (Task 5)



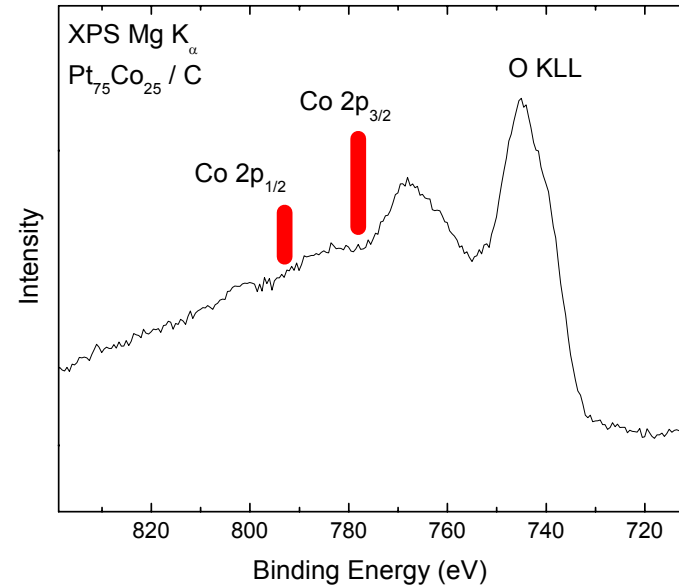
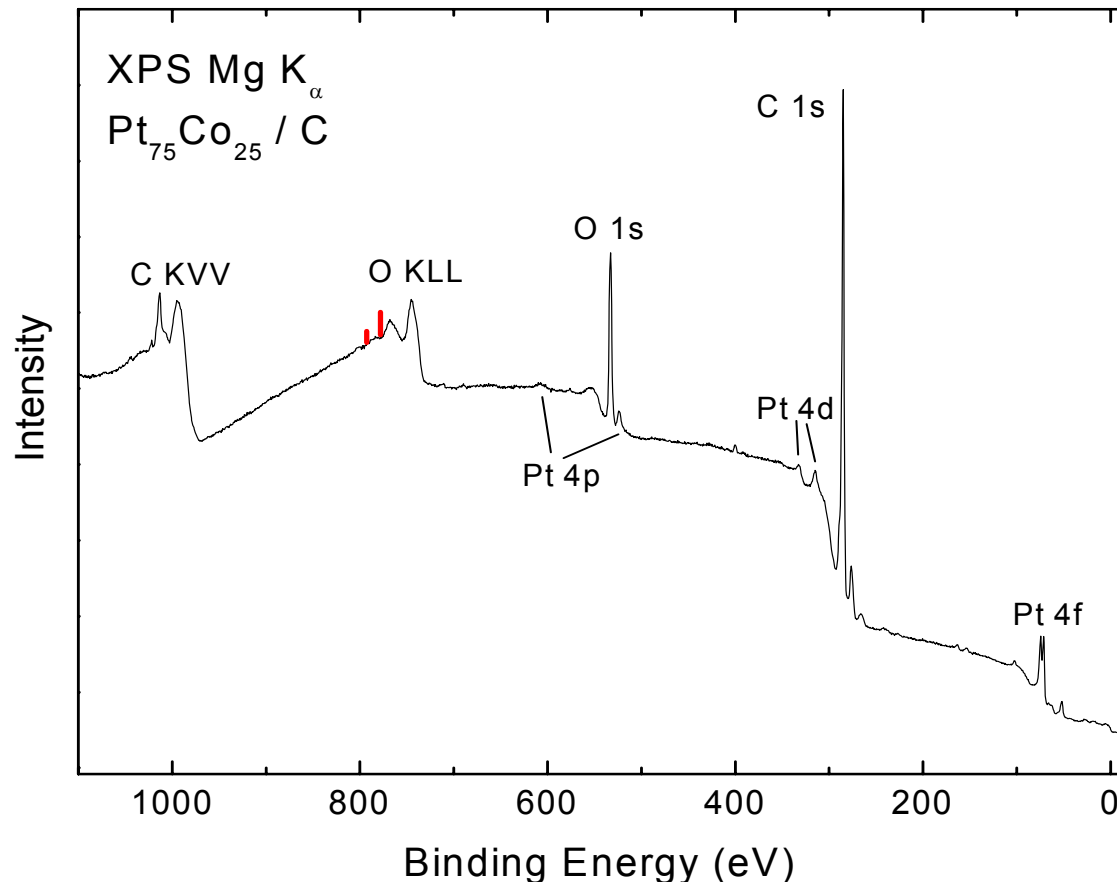
Comparison of Hirshfeld charges of Pt₃Co and Pt₃Co-C₂₄H₁₂

Hirshfeld Charges			
Pt₃Co			
Pt ₁	Pt ₂	Pt ₃	Co
-0.060	-0.050	-0.058	0.168

Hirshfeld Charges			
Pt₃Co-C₂₄H₁₂			
Pt ₁	Pt ₂	Pt ₃ *	Co*
-0.075	-0.078	0.065	0.106

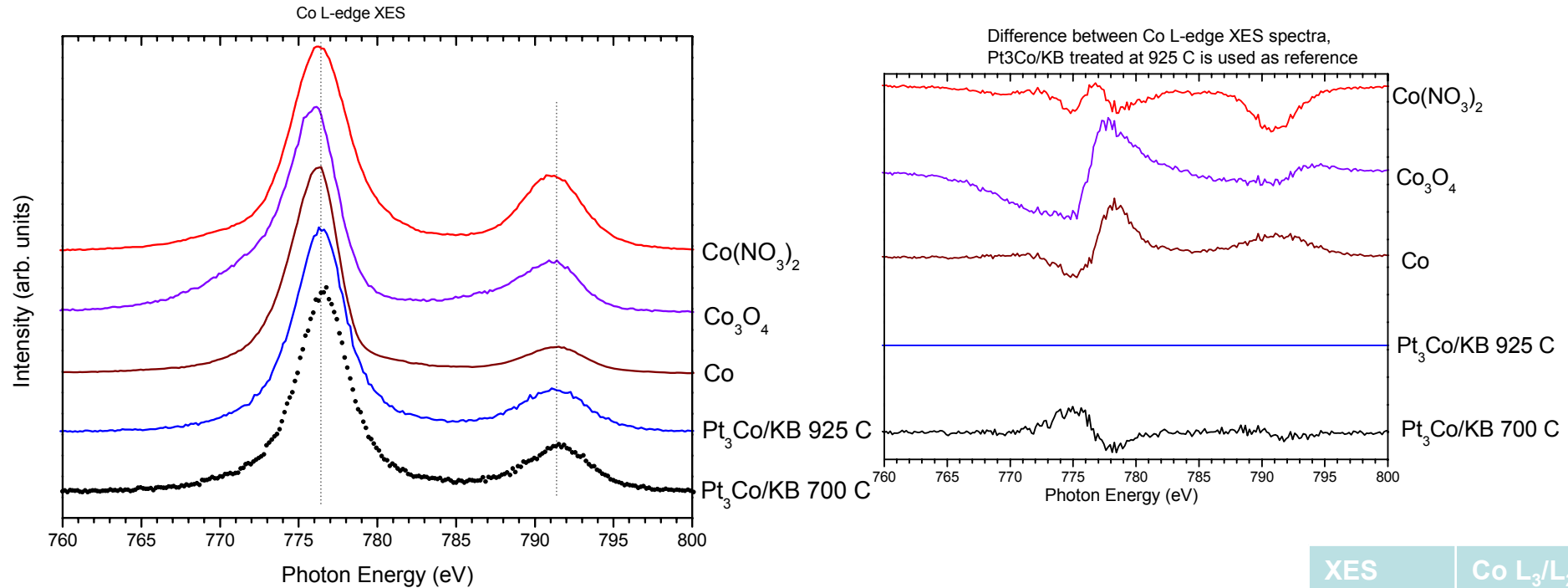
- Strong charge transfer occurs between Coronene and Pt₃Co cluster
- Coronene acts as an electron reservoir

First experiment: XPS of “off-the-shelf” Pt₃Co catalyst (Task 5)



- XPS survey spectrum shows the lines of Pt and C (as expected)
- In addition O 1s and O KLL can be observed due to adsorbates and/or oxidation of the surface
- No Co lines can be found (the red lines indicate position and intensity of the Co 2p lines if the Pt:Co **surface** stoichiometry would be 3:1) => no Co at the sample surface (independent of annealing temperature). BUT: XES clearly shows Co. Core-shell structure!

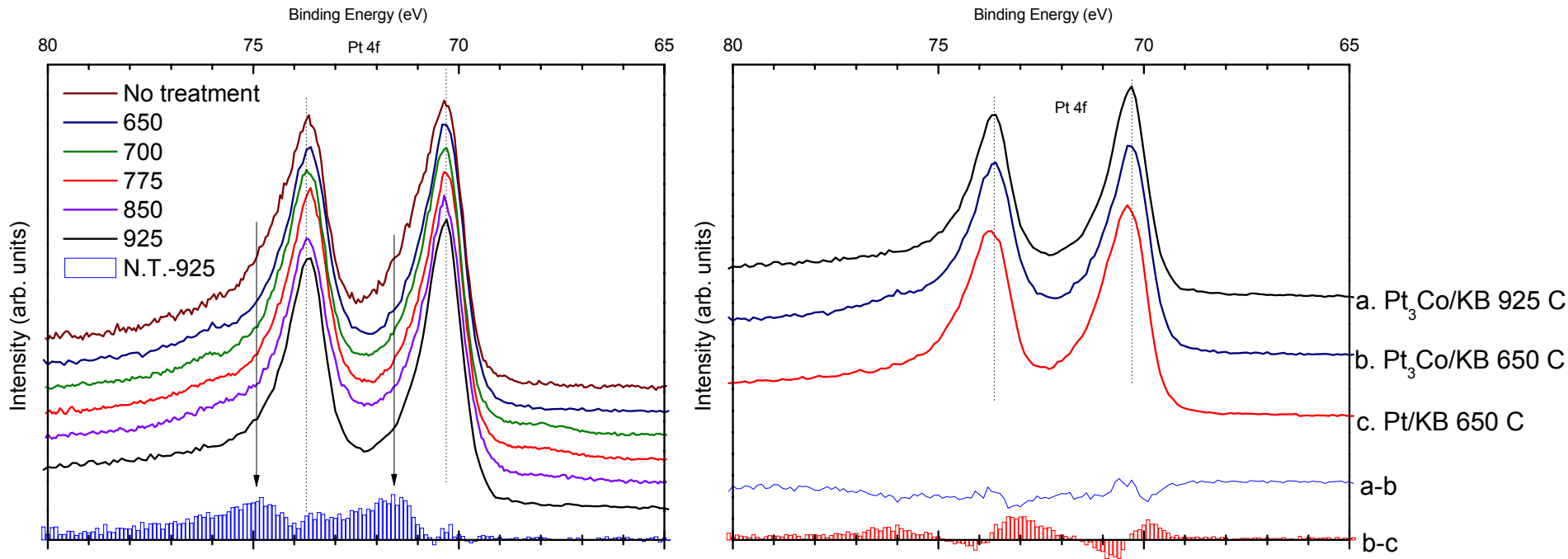
Co L-edge XES data: comparison with reference compounds (Task 5)



1. Co 3d unoccupied (XAS – not shown) and occupied states change with annealing temperature
2. Increasing the annealing temperature converts $\text{Co}(\text{NO}_3)_2$ into Co metal (or CoO_x)
3. Co L_3/L_2 ratio decreases at higher annealing temperature, but is still higher than the value of Co foil \Rightarrow information about Co density

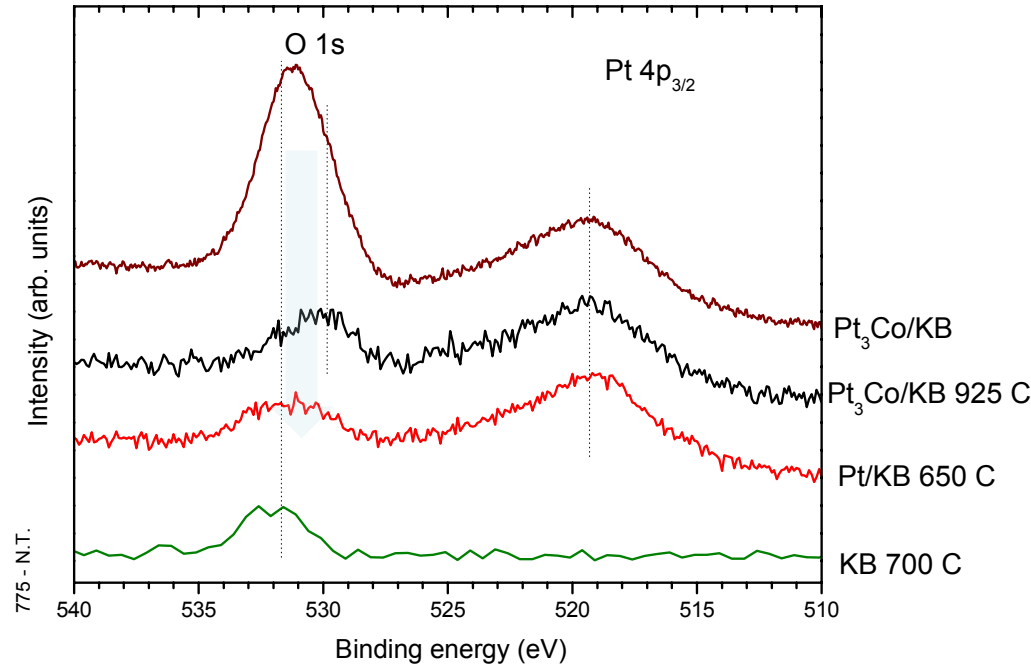
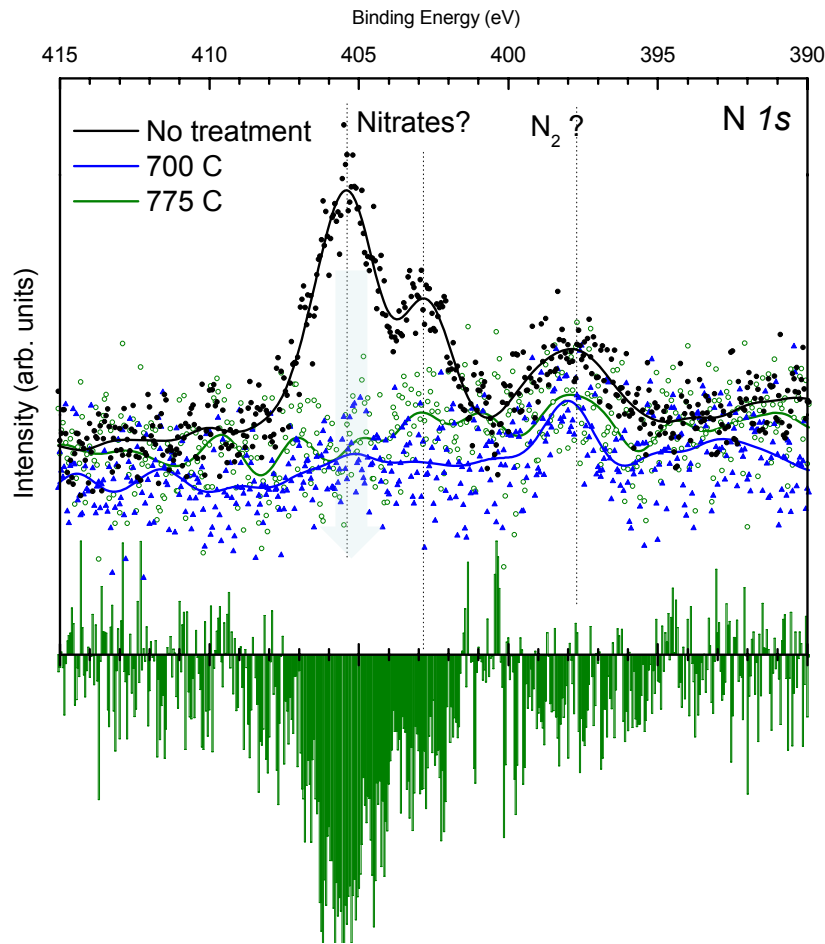
XES data	Co L_3/L_2
$\text{Co}(\text{NO}_3)_2$	0.38
Co_3O_4	0.26
Co foil	0.14
$\text{Pt}_3\text{Co}/\text{KB}$ 925 C	0.23
$\text{Pt}_3\text{Co}/\text{KB}$ 700 C	0.25

Pt 4f core level XPS (Task 5)



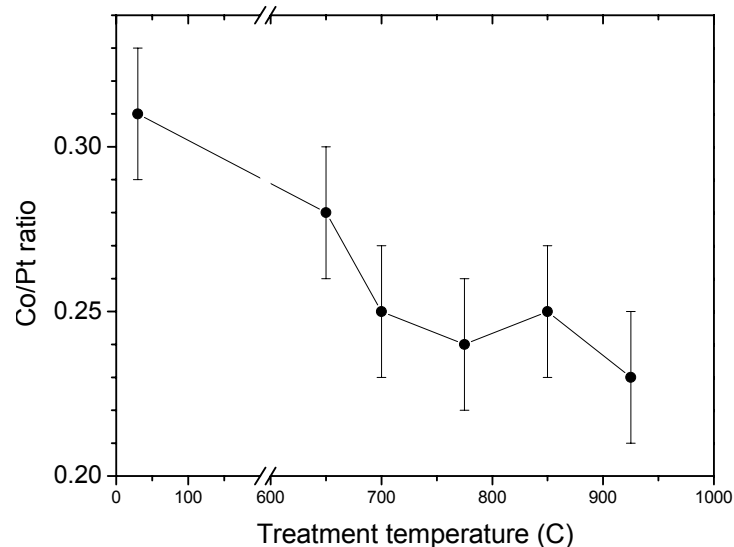
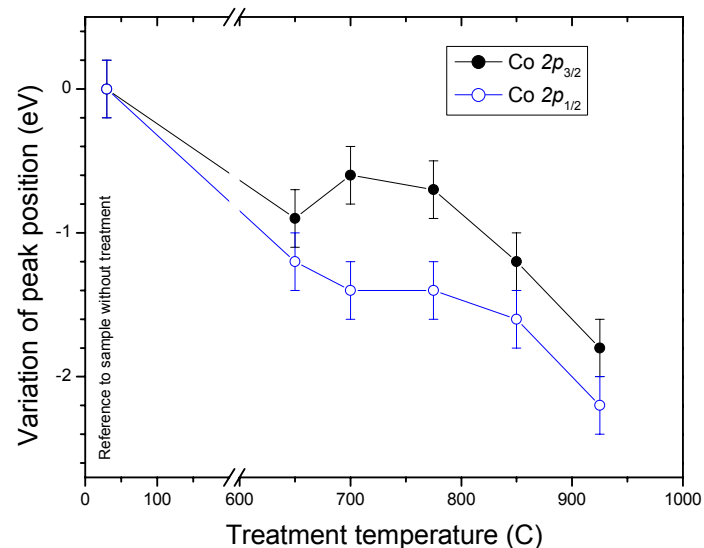
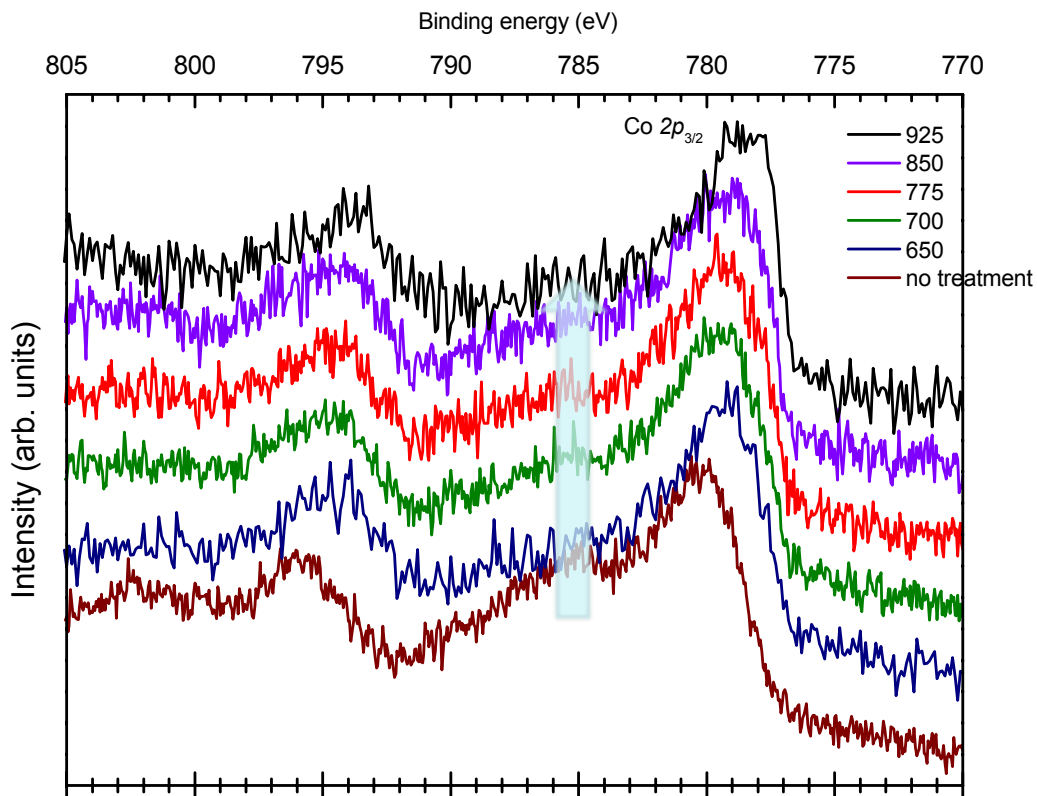
1. Pt 4f features indicates that most of the Pt is in metallic form, but a chemically different species is present for the “no-treatment” sample (presumably oxide or hydroxide)
2. At the same annealing temperature (650 C), Pt 4f from Pt₃Co/KB is slightly different than for the Pt/KB sample \Rightarrow indicates change in electronic environment due to Co incorporation
3. Annealing Pt₃Co/KB at 925 vs. 650 C also induces slight change in the electronic environment, presumably due to transition from $\text{Co}(\text{NO}_3)_2$ to Co (or CoO_x)

N 1s, O 1s, Pt 4p core level XPS (Task 5)



1. N 1s from Pt₃Co/KB samples changes greatly before and after anneal. This indicates a change of nitrate precursor concentration at the surface.
2. No nitrate at the surface after 700 C annealing.
3. The spectral intensity of O 1s decreases after annealing. Its spectral shape also changes, due to change of O chemical environment.

Co 2p core level XPS (Task 5)



1. Co 2p core levels visible for all samples (not “off-the-shelf”!)
2. They shift with increasing annealing temperature (reduction in oxide?)
3. Spectral intensity around 785 eV is suppressed after anneal (removal of nitrate?)

Summary for fuel cell catalyst studies (Task 5)

1. While earlier studies on “off-the-shelf” catalysts indicate the absence of Co on the surface, “fresh” samples show Co at all annealing temperatures. The Co/Pt ratio gradually decreases with annealing temperature
2. Annealing reduces precursor phases (i.e., nitrites) and contaminations (i.e., oxides), and gradually transforms Co and Pt into their metallic form
3. This transformation is not fully complete even at high anneal temperature – some oxides remain
4. Electronic structure calculations of Co doped Pt clusters show charge transfer from Co to Pt leading to increased charge polarization of the cluster and higher reactivity toward H₂, O₂, and CO adsorption
5. Preliminary results of Pt₄ and Pt₃Co cluster deposition on carbon substrates (coronene) indicate charge transfer from the electron rich substrate to the metal cluster

Future Work

Task 1

- Simultaneous co-evaporation of Ti and Li on the various carbon nanomaterials
- STM and STS of Ti and Li and H₂/H on carbon nanomaterials
- Li loading and hydrogen sorption studies of proposed carbon nanoframeworks
- Calculations of energy profiles (kinetics) of hydrogen adsorption and desorption on pure and alloyed Ti clusters and Ti-doped nanomaterials
- Explore properties of hydrogen multicenter bonds to design novel nanomaterials for hydrogen storage
- Investigate electronic structure and hydrogen storage properties of doped carbon nanofoams jointly with Yakobson (Rice)

Future Work

Task 3

- Examine stability of the materials as a function of repeated sorption cycles.
- Examine the role of sodium borohydride in the reduction of the chemical composites and enhancement of sorption properties.
- Have external sorption measurements performed? (\$\$\$\$)
- Examine the catalysis of the electrochemical PANI/Pd(IV) material.

Task 4

- Perform synthesis and characterization of partially fluorinated sulfonated copolyamides as potential high temperature PEM for fuel cells
- Perform joint experimental and theoretical studies of proton transport and electronic structures of the membrane material

Task 5

- In-situ annealing (in new photoemission system at UNLV, in new in-situ end-station at ALS!)
- Optimize UTC-like annealing processes at UNLV
- Perform calculations of catalyst support interactions with amorphous carbon support
- Perform electronic structure calculations of Pt-Co and Pt-Co-Ir alloy catalysts from UTC to complement ongoing experimental work at UNLV

Summary

- Joint experimental and theoretical work performed on electronic structure of carbon nanoclusters
- Stable structures of graphitic-BC₂N as potential hydrogen storage media identified
- The electronic structure of Ti decorated SWCNTs explored using X-ray and electron spectroscopy. Significant oxidation of Ti leading to TiO₂ formation is observed
- Systematically explored hydrogen uptake of transition metal-bonded organometallic systems (Sc, Ti, V) using DFT methods
- Proposed new class of carbon nanoframeworks (thin SWCNTs linked by phenyl spacers) as potential hydrogen storage media
- Investigated electronic structures and bondings in hydrogen saturated Ti and Ti-Al clusters and identified novel bonding motifs which may be harnessed to design novel hydrogen storage systems
- Synthesized bulk quantities of mesoporous PANI/Pd composites for hydrogen storage
- All experimental and computational capabilities are in place
- Published over 20 peer-reviewed manuscripts in leading journals